Renewable and Sustainable Energy Reviews 38 (2014) 348–367

Contents lists available at ScienceDirect

Renewable and Sustainable Energy Reviews

journal homepage: www.elsevier.com/locate/rser

Nanofluids for improved efficiency in cooling solar collectors – A review

Ali Najah Al-Shamani [a,b,*], Mohammad H. Yazdi [a], M.A. Alghoul [a], Azher M. Abed [a], M.H. Ruslan [a], Sohif Mat [a], K. Sopian [a]

[a] Solar Energy Research Institute (SERI), Universiti Kebangsaan Malaysia, 43600 Bangi, Selangor, Malaysia
[b] Department of Machinery Equipment Engineering Techniques, Technical College Al-Musaib, Foundation of Technical Education, Baghdad, Iraq

ARTICLE INFO

Article history:
Received 24 December 2013
Received in revised form
11 April 2014
Accepted 17 May 2014
Available online 21 June 2014

Keywords:
Nanofluids
Photovoltaic/thermal (PV/T)
Absorber collector
Performance
Exergy
Thermal and electrical efficiency

ABSTRACT

The use of nanofluids for cooling is an attracting considerable attention in various industrial applications. Compared with conventional fluids, nanofluids improve the heat transfer rate, as well as the optical properties, thermal properties, efficiency, and transmission and extinction coefficients of solar systems. The effects of different nanofluids on the cooling rate and hence the efficiency of solar systems can be experimentally investigated. Accordingly, this review paper presents the effects of nanofluids on the performance of solar collectors from the considerations of efficiency and environmental benefits. A review of literature shows that many studies have evaluated the potential of nanofluids for cooling different thermal systems. The second part of this paper presents an overview of the research, performance, and development of photovoltaic/thermal (PV/T) collector systems. Descriptions are made on water PV/T collector types, analytical and numerical models, and simulation and experimental works. The parameters affecting PV/T performance such as covered versus uncovered PV/T collectors, absorber plate parameters, and absorber configuration design types are extensively discussed. Exergy analysis shows that the coverless PV/T collector produces the largest total (electrical + thermal) exergy. Furthermore, PV/T collectors are observed to be very promising devices, and further work should be carried out to improve their efficiency and reduce their cost. Therefore, using nanofluids for cooling PV/T systems may be reasonable.

Contents

1. Introduction . . . 349
2. Performance thermal properties of nanofluids . . . 349
3. Enhancement heat transfer using nanofluids . . . 350
4. Performance of solar collector using nanofluids . . . 354
   4.1. Flat plate solar collector . . . 354
   4.2. Direct absorption solar collector . . . 355
   4.3. Evacuated tube solar collector . . . 356
   4.4. Parabolic trough collector . . . 356
   4.5. Concentrated-parabolic solar collectors . . . 357
5. PV/T collector . . . 357
6. Water-type PV/T collector . . . 357
   6.1. Glazed and unglazed . . . 357
   6.2. Performance of PV/T collector . . . 361
   6.3. Design absorber of PV/T collector . . . 362
   6.4. Exergy and energy analysis of PV/T collector . . . 364
7. Conclusion . . . 365
References . . . 366

* Corresponding author at: Solar Energy Research Institute, University Kebangsaan Malaysia, 43600 Bangi, Selangor, Malaysia.
E-mail addresses: ali.alshmani@yahoo.com, ali.alshamani@siswa.ukm.edu.my (A.N. Al-Shamani), mohammadhossein.yazdi@gmail.com (M.H. Yazdi).

http://dx.doi.org/10.1016/j.rser.2014.05.041
1364-0321/

1. Introduction

The advent of the oil crisis in the early 1970s and the global environment concerns in the 90s forced many to look for renewable and alternative clean energy sources. Therefore, an ingenious method of solar energy conversion must be developed and used as an alternative in the most vulnerable applications of fossil fuels. Biomass, solar energy, and wind energy are the world's most abundant permanent sources of energy; they are also important and environmentally compatible sources of renewable energy [1].

Energy is a thermodynamic quantity that is often understood as the capacity of a physical system to perform the work. Aside from its physical meaning, energy is vital for our relations with the environment. Life is directly affected by its energy and consumption. Energy resources based on fossil fuels are still dominant with the highest share in global energy consumption; however, clean energy generation is crucial because of the growing significance of environmental issues. Solar power is a key item in clean energy technologies because it provides an unlimited, clean, and environmentally friendly energy. Moreover, the other forms of renewable energy primarily depend on the incoming solar radiation. The Earth absorbs approximately 3.85 million EJ of solar energy per year [2].

Nanotechnology has an important function in promoting technology. Nanofluids are a mixture of liquid (base fluid) and nanoparticles (nanometer sized material) [3]. Nanofluids have intensified thermophysical properties, such as thermal conductivity, viscosity, and convective heat transfer coefficients, compared with conventional fluids [4]. A new and simple way to improve the performance of solar collector is to use nanofluids in place of conventional heat transfer fluids. Several articles have investigated the thermal conductivity of nanofluids to increase heat transfer rate. However, studies investigating the other properties of nanofluids, such as the effect of Brownian motion, and analyses based on two-phase fluid (suspended solid into liquid), are lacking.

Photovoltaic/thermal (PV/T) systems are a combination of photovoltaic (PV) and solar thermal component systems that produce both electricity and heat from the integrated component or system. PV/T technologies have a great potential for energy savings, and further work should be focused on reducing the cost and improving the efficiency of these technologies. PV/T technologies are expected to become strongly competitive with the conventional power generation in the near future. The first works on water PV/T collectors were presented by Kern and Russell [5]. The development of hybrid solar energy collectors that convert solar radiation into a balance of low-grade thermal energy and direct-current electricity was discussed. Five hybrid heating and cooling system configurations (baseline solar heating system, a parallel heat pump system, a series heat pump system, an absorption-cycle chiller, and a high-performance series advanced heat pump) were analyzed for four climatic cities in the USA. Cost analysis was also conducted to identify systems with optimum economics. The greatest potential energy savings in all four geographic regions are offered by an advanced heat pump system.

The effects of using different nanofluids on the cooling rate and hence the efficiency of PV/T systems can be investigated experimentally. In this area, the effects of different volume fractions and nanoparticle sizes on the efficiency of the system can be studied. Cooling the PV cell and decreasing its temperature are necessary to obtain more power and heat from the PV/T system. An affective cooling strategy of PV/T panels is currently lacking. There is a strong motivation to improve advanced heat transfer fluids with substantially higher thermal conductivity called nanofluids. Using nanofluids instead of conventional fluid improves heat transfer as well as the optical and thermal properties, performance, and efficiency of the PV/T collector.

2. Performance thermal properties of nanofluids

Thermal conductivity is an important parameter in enhancing the heat transfer performance of a heat transfer fluid. The thermal conductivity of solid metals is higher than that of fluids; hence, suspended particles are expected to be capable of increasing thermal conductivity and heat transfer performance. Many researchers have reported experimental studies on the thermal conductivity of nanofluids. The transient hot wire method, temperature oscillation, and the steady-state parallel plate method have been used to measure the thermal conductivity of nanofluids. SiO_2, Al_2O_3, and CuO are the most commonly used nanoparticles in experiments. Even when the size of the particles and the type of base fluids are different, all experimental results showed enhancement in thermal conductivity.

Wang et al. [6] investigated the effective thermal conductivity of mixtures of fluids and nanometer-sized particles by a steady-state parallel-plate method. Base fluids [water, ethylene glycol (EG), vacuum pump oil, and engine oil] contained suspended Al_2O_3 and CuO nanoparticles with average diameters of 28 and 23 nm, respectively. Possible mechanisms underlying the enhancement of the thermal conductivity of the mixtures were discussed. Experimental results show that the thermal conductivities of nanofluid mixtures are higher than those of base fluids. Thus, existing models are not suitable for use in nanofluid mixtures.

Eastman et al. [7] measured the thermal conductivity of nanofluids containing Al_2O_3, CuO, and Cu nanoparticles with two base fluids, namely, water and HE-200 oil by suspending nanocrystalline particles in the liquid to produce nanofluids. In the case of oxide nanoparticles suspended in water, increases in thermal conductivity of approximately 60% can be obtained with 5 volume % particles. The use of Cu nanoparticles results in even larger improvements in thermal conductivity behavior, with very small concentrations of particles producing major increases in the thermal conductivity of oil.

Lee et al. [8] studied the thermal conductivity of fluids containing oxide nanoparticles, suspended CuO (18.6 and 23.6 nm) and Al_2O_3 (24.4 and 38.4 nm) with two base fluids, namely, water and EG. They obtained four combinations of nanofluids: CuO in water, CuO in EG, Al_2O_3 in water, and Al_2O_3 in EG. They found that nanofluids have substantially higher thermal conductivities than the same liquids without nanoparticles. The CuO/EG mixture showed an enhancement of more than 20% at 4 vol% of nanoparticles. In the low-volume fraction range (< 0.05 in test), the thermal conductivity ratios increase almost linearly with volume fraction. Although the size of Al_2O_3 nanoparticles is smaller than that of CuO, CuO-nanofluids exhibit higher thermal conductivity values than Al_2O_3-nanofluids.

Xuan and Li [9] introduced a procedure for preparing nanofluid suspension consisting of nanophase powders and a base liquid. Sample nanofluids were prepared using this procedure. A theoretical study of the thermal conductivity of nanofluids was introduced. Factors such as the volume fraction, dimensions, shapes, and properties of the nanoparticles were discussed. A theoretical model was proposed to describe the heat transfer performance of nanofluids flowing in a tube while accounting for the dispersion of solid particles. They found that the thermal conductivity of nanofluids increases with the volume fraction of ultra-fine particles.

Eastman et al. [10] attempted to increase the effective thermal conductivities of EG-based nanofluids containing copper nanoparticles. They used pure Cu nanoparticles < 10 nm in size and achieved a 40% increase in thermal conductivity for only 0.3% volume fraction of the solid dispersed in EG. They indicated that the increased ratio of surface to volume with decreasing size should be an important factor. They also showed that the additive

acid may stabilize the suspension and thus increase the effective thermal conductivity.

Xie et al. [11] investigated the thermal conductivity of Al_2O_3 nanoparticle suspensions using a transient hot-wire method with specific surface areas (SSA) in a range of 5–124 m^2/g. The addition of nanoparticles into the fluid increased the thermal conductivity. The enhanced thermal conductivity increases with increasing difference between the pH of the aqueous suspension and the isoelectric point of the Al_2O_3 nanoparticles. Comparison between the experiments and the theoretical model shows that the measured thermal conductivity is much higher than the values calculated using theoretical correlation.

Das et al. [12] investigated the effect of temperature on thermal conductivity enhancement for nanofluids containing Al_2O_3 and CuO through an experimental investigation using temperature oscillation. They observed a twofold to fourfold increase in thermal conductivity over the temperature range of 21–52 °C. The results suggest that nanofluids can serve as cooling fluids for devices with high energy density at temperatures higher than room temperature.

Hong and Yang [13] investigated the enhanced thermal conductivity of Fe nanofluids with EG. Fe nanoparticles with a mean size of 10 nm were produced by chemical vapor condensation. They found that Fe nanofluids exhibit a higher enhancement of thermal conductivity than Cu nanofluids. Their result indicated that materials with high thermal conductivity are not always the best candidates for the suspension to improve the thermal characteristics of base fluids. They concluded that the thermal conductivity of nanofluids increases nonlinearly with the solid volume fraction.

Murshed et al. [14] prepared TiO_2 suspension in water using the two-step method in spherical shapes of 15 nm in deionized water. A transient hot-wire apparatus with an integrated correlation model was used to measure the thermal conductivities of these nanofluids more conveniently. The experimental results show that the thermal conductivity increases with increasing particle volume fraction. The particle size and shape also affect the enhancement of thermal conductivity.

Li and Peterson [15] presented an experimental investigation to examine the effects of different temperatures and volume fractions on the effective thermal conductivity of CuO and Al_2O_3 water suspensions. They found that nanoparticle material, diameter, volume fraction, and bulk temperature significantly affect the thermal conductivity of nanofluids. For Al_2O_3/water, an increase in the mean temperature from 27 °C to 34.7 °C increases the thermal conductivity by nearly three times.

Hwang et al. [16] investigated the characteristics of thermal conductivity enhancement of nanofluids. Four types of nanofluids, such as multiwalled carbon nanotubes (MWCNTs) in water, CuO in water, SiO_2 in water, and CuO in EG, were produced. The thermal conductivity enhancement of water-based MWCNT nanofluid increased by up to 11.3% at a volume fraction of 0.01. They found that the thermal conductivity enhancement of nanofluids depends on the thermal conductivities of both particles and the base fluid.

Lee et al. [17] investigated the effective viscosities and thermal conductivities of water-based nanofluids containing very low concentrations of Al_2O_3 nanoparticles. They produced Al_2O_3–water nanofluids with various concentrations from 0.01 vol% to 0.3 vol%. The measured viscosities of the Al_2O_3–water nanofluids show a nonlinear relation to the concentration even in the low-volume concentration (0.01–0.3%) range. The measured thermal conductivities of the Al_2O_3–water nanofluids increase nearly linearly with the concentration.

Vajjha and Das [18] investigated the thermal conductivity of three nanofluids containing aluminum oxide, copper oxide, and zinc oxide nanoparticles dispersed in a base fluid of 60:40 (by mass) EG and water mixture. Different particle volumetric concentrations of up to 10% were tested, and the temperature range of the experiments ranged from 298 K to 363 K. They found that the thermal conductivity of nanofluids increases compared with that of the base fluids as the volumetric concentration of nanoparticles increases. The thermal conductivity increases substantially with increasing temperature. The thermal conductivity decreases as the nanoparticle diameter increases. These new correlations give an accurate prediction of thermal conductivity of different nanofluids over a wide range of concentration and temperature. In conclusion, the applications of these nanofluids in higher temperature environment will be more beneficial as their thermal conductivity increases with increasing temperature.

Mintsa et al. [19] presented the effects of thermal conductivity measurements in alumina/water and copper oxide/water nanofluids. The effects of particle volume fraction, temperature, and particle size were investigated. Readings at ambient temperature as well as over a relatively large temperature range were made for various particle volume fractions up to 9%. They found the predicted overall effect of increasing effective thermal conductivity with increasing particle volume fraction and with decreasing particle size. The relative increase in thermal conductivity is more important at higher temperatures as well as with smaller diameter particles. From the above-mentioned discussion, which is also summarized in Table 1, we find that the available experimental data from different research groups vary widely. Further investigations are necessary to clarify the current predicament.

3. Enhancement heat transfer using nanofluids

Wen and Ding [20] investigated an experimental work on the convective heat transfer of nanofluids made of γ-Al_2O_3 nanoparticles and deionized water flowing through a copper tube in the laminar flow regime. They found that using Al_2O_3 nanoparticles as the dispersed phase in water can significantly enhance the convective heat transfer in the laminar flow regime. This enhancement in convective heat transfer increases with Reynolds number as well as particle concentration under the conditions of this work. The thermal developing length of nanofluids is greater than that of pure base liquid and increases with increasing particle concentration. The local heat transfer coefficient increases with particle concentration. As shown in Fig. 1, the heat transfer enhancement significantly decreases with increasing distance from the entrance region. For the nanofluid with 1.6% by volume nanoparticles, particle migration was proposed to be a reason for the enhancement, which results in a nonuniform distribution of thermal conductivity and viscosity field, and reduces the thermal boundary layer thickness.

Zhou [21] investigated heat transfer characteristics of copper nanofluids with and without acoustic cavitation. The effects of such factors as acoustical parameters, nanofluids concentration, and fluid subcooling on heat transfer enhancement around a heated horizontal copper tube were discussed. Independent of Cu nanoparticles, the effects of acoustic cavitation and fluid on heat transfer characteristics of the tube remain unchanged. Whether or not convection heat transfer is enhanced by nanoparticles largely depends on thermophysical properties.

Yang et al. [22] presented the heat transfer properties of nanoparticle-in-liquid dispersions (nanofluids) measured under laminar flow in a horizontal tube heat exchanger. Graphitic nanoparticles with significantly different aspect ratios ($l/d=0.02$) were used in this study. The graphite nanoparticles increased the static thermal conductivities of the fluid significantly at low weight fraction loadings. The experimental heat transfer coefficients showed lower increases than predicted by either the

Table 1
Summary of experimental studies on thermal conductivity of nanofluids.

Investigator	Particles	Size (nm)	Fluids	Observations
Wang et al. [6]	Al_2O_3, CuO	28, 23	Water, ethylene glycol, pump oil, engine oil	12% Improvement from 3 vol% Al_2O_3/water nanofluids
Eastman et al. [7]	Al_2O_3, CuO, Cu	18, 33, 36	Water, E-200 oil	A 60% improvement from 5 vol% CuO particles in water
Lee et al. [8]	CuO Al_2O_3	18.6, 23.6. 24.4, 38.4	Water, ethylene glycol	The CuO/EG mixture showed enhancement of more than 20% at 4 vol% of nanoparticles
Xuan and Li [9]	Cu	100	Water, Oil	Successful suspension of relatively big metallic nanoparticles
Eastman et al. [10]	Cu	<10	Ethylene glycol	40% Increase from 0.3 vol% Cu-based nanofluids
Xie et al. [11]	Al_2O_3		Water	The thermal conductivity enhancements are highly dependent on the specific surface area (SSA) of the nanoparticle
Das et al. [12]	Al_2O_3, CuO	38.4/28.6	Water	2–4 Fold increase over range of (21–52) °C
Hong and Yang [13]	Fe	10	Ethylene glycol	18% Increase for 0.55 vol% Fe/EG nanofluids
Murshed et al. [14]	TiO_2	Rod⌀10 × 40, spherical⌀15	Deionized water	33% and 30% enhancement of the effective thermal conductivity occurred for TiO_2 particles of ⌀10 × 40 and ⌀15, respectively
Li and Peterson [15]	Al_2O_3, CuO	36, 29	Water	Enhancement with volume fraction and temperature
Hwang et al. [16]	MWCNT, SiO_2, CuO		Water, ethylene glycol	Enhancement of water-based MWCNT nanofluid was increased up to 11.3% at a volume fraction of 0.01
Lee et al. [17]	Al_2O_3	30 ± 5 nm	Water	Enhancement with volume concentration and temperature
Vajjha and Das [18]	Al_2O_3, CuO, ZnO	Up to 10	60:40 ethylene glycol: water mixture	The nanofluids exhibit enhanced thermal conductivity with an increase in temperature
Mintsa et al. [19]	Al_2O_3, CuO	Up to 9	Water	Increase in thermal conductivity is more important at higher temperatures as well as with smaller diameter particles

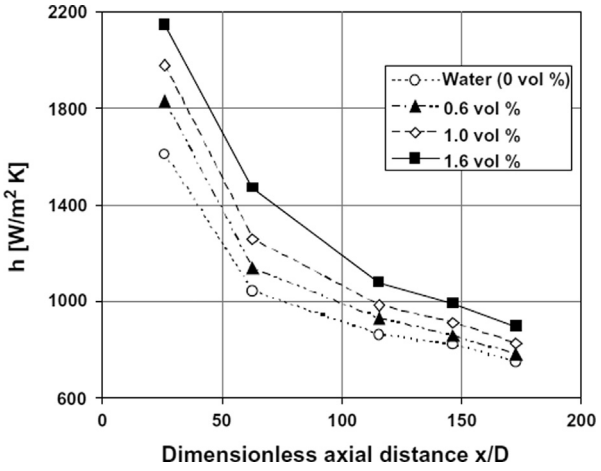

Fig. 1. Axial profile of local heat transfer coefficient (Re = 1050 ± 50) [20].

conventional heat transfer correlations for homogeneous fluids. As shown in Fig. 2, at 50 °C, nanofluids with higher loading (2.5 wt%) showed a 22% increase in heat transfer coefficient and an approximately 50% increase in thermal conductivity compared with the base fluid. At 70 °C, the heat transfer coefficient increases to 15%.

Ding et al. [23] presented the heat transfer behavior of aqueous suspensions of MWCNT nanofluids flowing through a horizontal tube. Significant enhancement in convective heat transfer was observed. The enhancement depends on the flow conditions (Re), CNT concentration, and pH, with pH eliciting the smallest effect. Given CNT concentration and pH, Ding et al. found a Re above which a significant increase in the convective heat transfer coefficient occurs. As shown in Fig. 3, for nanofluids containing 0.5 wt% CNTs, the maximum enhancement is over 350% at Re = 800, The observed large enhancement of the convective heat transfer could not be attributed purely to the enhancement of thermal conduction under static conditions.

Heris et al. [24] investigated the convective heat transfer of Al_2O_3/water nanofluid in laminar flow through circular tube with constant wall temperature boundary condition. The Nusselt numbers of nanofluids were obtained for different nanoparticle concentrations as well as various Peclet and Reynolds numbers.

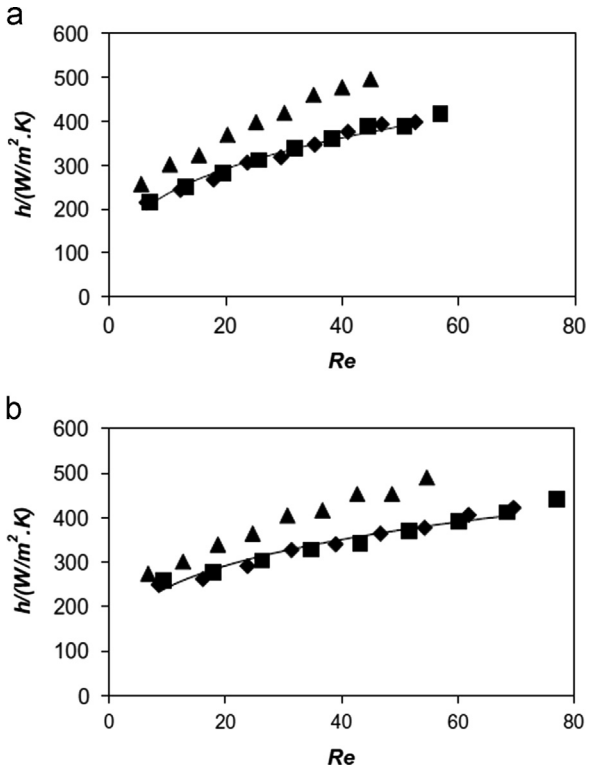

Fig. 2. Plot of heat transfer coefficient versus Reynolds number for Series 1 fluids (a) 50 °C, (b) 70 °C. (♦) Base fluid 1; (■) EF#1-1; (▲) EF#1-2; (—) fitting for BF#1 according to power law correlation [22].

The experimental results indicate that the heat transfer coefficient of nanofluids increases with Peclet number and nanoparticle concentration. They concluded that the increase in thermal conductivity is not the only reason for heat transfer enhancement in nanofluids. Particle fluctuations and interactions, especially in high Peclet number, may cause the change in flow structure and lead to augmented heat transfer because of the presence of nanoparticles.

Ding et al. [25] experimentally investigated convective heat transfer using aqueous and EG-based spherical titania nanofluids,

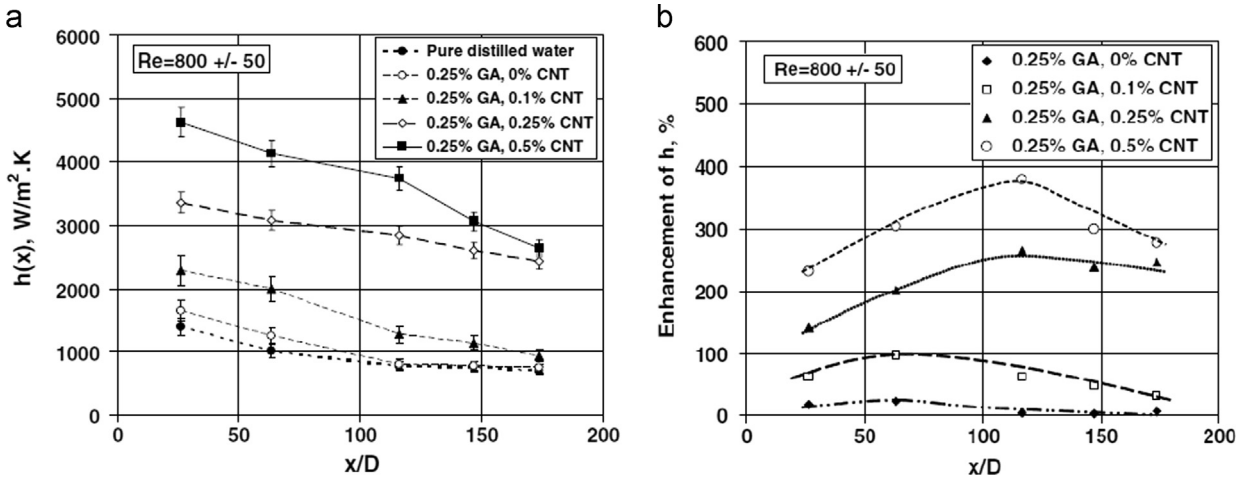

Fig. 3. Axial profiles of (a) heat transfer coefficient and (b) enhancement of heat transfer coefficient for different CNT concentrations (pH = ~6) [23].

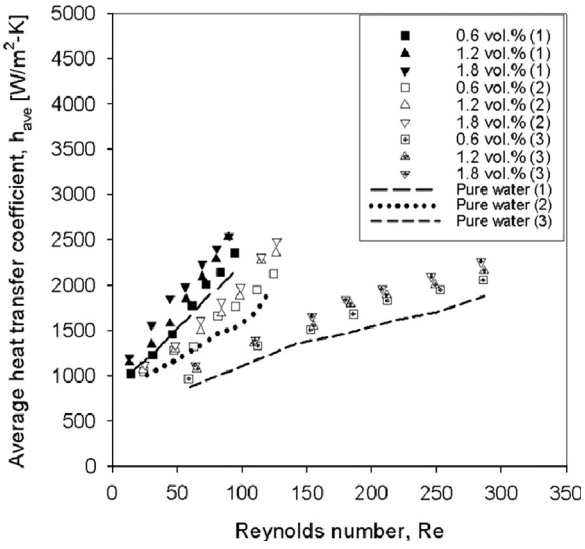

Fig. 4. Heat transfer coefficient versus Reynolds number [26].

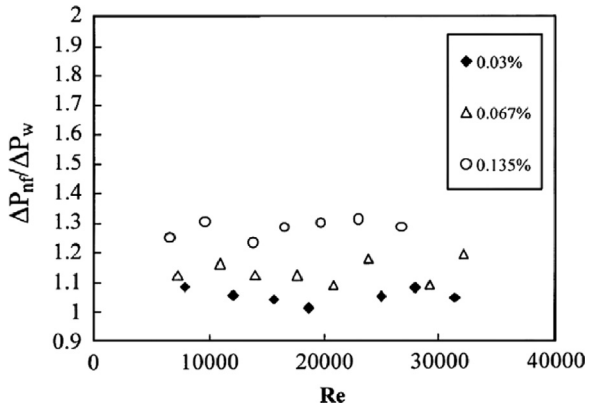

Fig. 5. The ratio of experimental pressure drop of nanofluids to that of pure water along the test tube versus Reynolds number at different volume concentrations [27].

aqueous-based titanate nanotubes, CNTs, and nano-diamond nanofluids. These nanofluids were formulated from dry nanoparticles and pure base liquids to eliminate complications caused by unknown solution chemistry. Except for the EG-based titania nanofluids, all other nanofluids were found to be nonNewtonian. For aqueous-based titania and carbon and titanate nanotube nanofluids, the convective heat transfer coefficient enhancement exceeds. Possible mechanisms for the observed controversy were discussed from both microscopic and macroscopic viewpoints. The competing effects of particle migration on the thermal boundary layer thickness and that on the effective thermal conductivity were suggested to be responsible for the experimental observations.

Jung et al. [26] investigated the convective heat transfer coefficient and friction factor of nanofluids in rectangular microchannels. An integrated microsystem consisting of a single microchannel on one side, as well as two localized heaters and five polysilicon temperature sensors along the channel on the other side, was fabricated. Aluminum dioxide (Al_2O_3) with 170 nm-diameter nanofluids with various particle volume fractions was used to investigate the effect of nanoparticle volume fraction on the convective heat transfer and fluid flow in microchannels. Fig. 4 shows the heat transfer coefficients versus Reynolds numbers of pure water, various nanofluids, and different microchannels. The heat transfer coefficients of all nanofluids are greater than those of their base fluids (i.e., pure water). They found that the Nusselt number increases with increasing Reynolds number in the laminar flow regime. The measured Nusselt number, which is less than 0.5, was successfully correlated with Reynolds number and Prandtl number based on the thermal conductivity of nanofluids.

Fotukian and Esfahany [27] investigated turbulent convective heat transfer and pressure drop of γ-Al_2O_3/water nanofluid inside a circular tube. The volume fraction of nanoparticles in base fluid was less than 0.2%. Results show that the addition of small amounts of nanoparticles to the base fluid remarkably augments heat transfer. Increasing the volume fraction of nanoparticles in the range studied in this work did not significantly affect heat transfer enhancement. Fig. 5 shows the ratio of the pressure drop of nanofluids to that of pure water as a function of Reynolds number. In this work, the addition of nanoparticles to the base fluid significantly increased the pressure drop. The pressure drop of nanofluids increased as the volume fraction of nanoparticles increased. Comparison between experimental results with existing correlations for convective heat transfer coefficients of nanofluids showed that experimental results well agreed with Maiga's correlation.

Fotukian and Esfahany [28] investigated experimentally turbulent convective heat transfer performance and pressure drop of dilute CuO/water nanofluid flowing through a circular tube. The heat transfer coefficient increased by approximately 25% compared with pure water. To better understand the effect of Reynolds number and nanoparticle concentration on the heat transfer performance of nanofluids, the ratio of the convective heat

transfer coefficient of nanofluids to that of pure water as a function of Reynolds number is plotted in Fig. 6. The heat transfer coefficient can be significantly changed by suspending a small amount of nanosized CuO particles in water. The pressure drop of nanofluids increases as the volume fraction of nanoparticles increases. Flow resistance significantly increased compared with the base fluid even at very low concentrations of CuO.

Sajadi and Kazemi [29] experimentally studied the turbulent heat transfer behavior of titanium dioxide/water nanofluids in a circular pipe where the volume fraction of nanoparticles in the base fluid was less than 0.25%. Experimental measurements were carried out in the fully developed turbulent regime for various volumetric concentrations. They found that adding a small amount of TiO_2 nanoparticles increases the heat transfer coefficient of nanofluids. The rate of the heat transfer coefficient enhancement of nanofluids to that of pure water decreased with increasing Reynolds number. The pressure drop of nanofluids increased as the volume fraction of nanoparticles increased. The experimental data contradict with existing correlations for the Nu of nanofluids developed in previous studies.

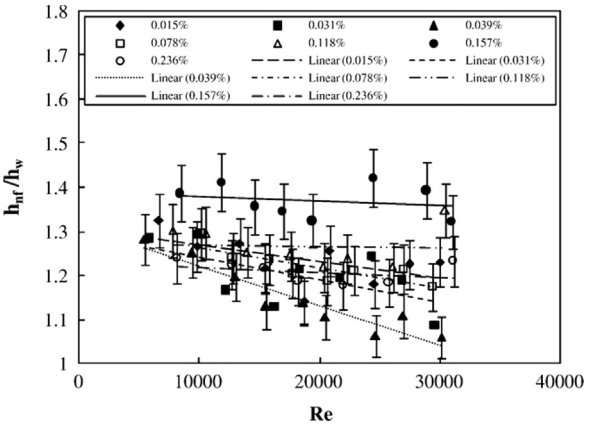

Fig. 6. The ratio of experimental heat transfer coefficient of nanofluids to pure water versus Reynolds number at different loadings of nanoparticles [28].

Akhavan-Behabadi et al. [30] presented the heat transfer enhancement of nanofluid flow inside vertical helically coiled tubes in the thermal entrance region. The temperature of the tube wall was kept constant at approximately 95 °C to have the isothermal boundary condition. The effects of a wide range of different parameters, such as Reynolds numbers, geometrical parameters, and nanofluid weight fractions, were studied. Based on the experimental data, utilizing helical coiled tubes instead of straight ones enhances the heat transfer rate remarkably. Nanofluid flows have higher Nusselt numbers compared with the base fluid flow. The combination of the two methods can remarkably enhance the heat transfer rate.

Kayhani et al. [31] performed an experimental study of convective heat transfer and pressure drop of turbulent flow of TiO_2–water nanofluid through a uniformly heated horizontal circular tube. Spherical TiO_2 nanoparticles with a nominal diameter of 15 nm were fictionalized by a new chemical treatment and then dispersed in distilled water to form stable suspensions containing 0.1%, 0.5%, 1.0%, 1.5%, and 2.0% volume concentrations of nanoparticles. They found that heat transfer coefficients increase as the volume fraction of the nanofluids increases but remain unchanged at different Reynolds numbers. Comparison between experimental results with existing correlations for convective heat transfer coefficients and pressure drop of nanofluids showed that experimental results agree with the correlations.

As shown in Table 2, the heat transfer coefficient increased with increasing Reynolds number, Nusselt number, and volume fraction of nanofluids.

Table 2
Summary of studies on heat transfer of nanofluids.

Author	Particles	Size (nm)	Volume fraction (vol%)	Base fluids	Result
Wen and Ding [20]	γ-Al_2O_3	26–56 nm	0.6, 1, 1.6	Water	For the nanofluids with 1.6%, HTC is 41% and 47% higher at Re=1050, 1600 respectively in comparison with the case of water only
Zhou [21]	Cu	80–100 nm	0–0.4 g/l	Acetone	Convection heat transfer enhanced due to the addition of a small amount of Cu nanoparticles
Yang et al. [22]	Graphite	20–40 nm	2–2.5	Oil	For (2.5 wt%) HTC at 50 °C increase of 22% over basefluid, at 70 °C increase averages 15%
Ding et al. [23]	CNT	100 nm	0–1 wt%	Water	For nanofluids 0.5 wt% CNTs, the maximum enhancement over 350% at Re=800, and the maximum enhancement occurs at an axial distance of approximately 110 times the tube diameter
Heris et al. [24]	Al_2O_3 CuO	20 nm 50–60 nm	0.2–3.0 wt%	Water	Heat transfer coefficient of nanofluids increases with Peclet number as well as nanoparticles concentration
Ding et al. [25]	TiO_2, TNT, CNT, ND particles	20 nm 10 nm, D=100 nm, L=2–50 nm	0–4.0 wt%	Aqueous Ethylene glycol	For aqueous-based Titania and carbon and titanate nanotubes nanofluids, the convective heat transfer coefficient enhancement exceeds, by a large margin, the extent of the thermal conduction enhancement
Jung et al. [26]	Al_2O_3	170 nm	0.6–1.6 wt%	Water	The HTC of the Al_2O_3 nanofluid in the laminar flow regime increased up to 32% compared to the pure water at 1.8 wt%
Fotukian and Esfahany [27]	γ-Al_2O_3	20 nm	0.03, 0.054, 0.067, 0.135	Water	The maximum value of 48% increase in HTC compared to pure water for 0.054%. The pressure drop of nanofluids with 0.135% volume concentration 30% increase at Reynolds number of 20,000 compared to pure water
Fotukian and Esfahany [28]	CuO	30–50 nm	Up to 0.24 wt%	Water	HTC increases 25% compared to pure water. The pressure drop of nanofluids increases 30% at Re=20, 000 compared to pure water. Increase flow resistance
Sajadi and Kazemi [29]	TiO_2	30 nm	0.05, 0.10, 0.15, 0.20, 0.25 wt%	Water	HTC increase 22 % and the maximum pressure drop about 25 % at Re=5000 for 0.25 wt% comparison with pure water
Akhavan-Behabadi et al. [30]	MWCNT	OD=5–20 nm ID=2–6 nm L=1–10 μm	0.1–0.4 wt%	Oil	HTC goes up as the nanofluid volume fraction or the Reynolds number increases. The Nu of nanofluids up to 60% higher than that for the base fluid
Kayhani et al. [31]	TiO_2	0.1, 0.5, 1, 1.5, 2 wt%	15 nm	Water	Nu increase by 8% at Re=11780 for nanofluid with 2 wt% HTC and pressure drop increase with increased volume fraction and Re

4. Performance of solar collector using nanofluids

The performance of a solar collector is described by an energy balance. Energy balance presents the distribution of incident solar radiation into useful energy gain, thermal losses, and optical losses. Thermal energy is lost from collector to the surroundings by conduction, convection, and radiation [32]. The performance of solar collector can be analyzed by following the procedure described by Hotteland Woertz [33] and extended by ASHRAE [34]. The basic equation is

$$Q_u = I_{t\theta}(\tau\alpha)_\theta - U_L(T_{p,m} - T_a) = \frac{\dot{m}\, C_p (T_{fe} - T_{fi})}{A_{ap}} \quad (1)$$

Eq. (1) may also be conformed for concentrating collectors [34]:

$$Q_u = I_{DN}(\tau\alpha)_\theta(\rho\Gamma) - U_L\left(\frac{A_{abs}}{A_{ap}}\right)(T_{abs} - T_a) \quad (2)$$

Different testing standards can be used to characterize the collector performance. Examples of such standards are ASHRAE-93; 2003, which is used in the USA, and EN-12975; 2006, which is used in European countries.

The steady-state thermal efficiency of a basic flat plate solar collector is calculated by Duffie and Beckman [32]

$$\eta = \frac{\int Q_u d_\tau}{A_c \int G_T d_\tau} \quad (3)$$

The useful energy output of a collector is the difference between the absorbed solar radiation and the thermal loss:

$$Q_u = A_c\left[S - U_L(T_{p,m} - T_a)\right] \quad (4)$$

where S is the solar energy absorbed by a collector, G_T is the incident solar energy, U_L is the heat transfer coefficient, $T_{p,m}$ is the mean absorber plate temperature, T_a is the ambient temperature, and A_c is the collector area.

In recent years, the numbers of experimental, theoretical, and numerical works on the application of nanofluids in solar collector have increased. In this paper, we present the experimental, theoretical, and numerical works had conducted by different authors for different types of solar collector along with the types and results of nanofluids.

4.1. Flat plate solar collector

Yousefi et al. [35] investigated experimentally the effect of Al_2O_3–water nanofluid as working fluid on the efficiency of a flat-plate solar collector (Fig. 7). The effects of mass flow rate, nanoparticle mass fraction, and surfactant on the efficiency of the collector were studied. The weight fractions of the nanoparticles were 0.2% and 0.4%, and the particle dimension was 15 nm. Experiments were performed with and without Triton X-100 as surfactant. The ASHRAE standard was used to calculate the efficiency. Compared with water as the absorption medium, the nanofluids as the working fluid increased the efficiency. In conclusion, the surfactant increases heat transfer. The maximum enhanced efficiency was 15.63% in the presence of the surfactant.

Yousefi et al. [36] investigated experimentally the effect of MWCNT nanofluid as absorbing medium on the efficiency of a flat-plate solar collector. The weight fractions of CNTs were 0.2% and 0.4%. Moreover, the effect of Triton X-100 as a surfactant on the stability of nanofluids was studied. They found that increasing the weight fraction from 0.2% to 0.4% can increase the efficiency. In addition, using the surfactant can increase also the efficiency. The increase in the efficiency depends on the temperature difference parameter $(T_i - T_a/G_T)$. However, for 0.4 wt% MWCNT nanofluid without surfactant, the efficiency also increased (Fig. 8). For small values of reduced temperature differences parameter, the efficiency can be increased by increasing the mass flow rate. Beyond these small values, the efficiency exhibits a reversed trend.

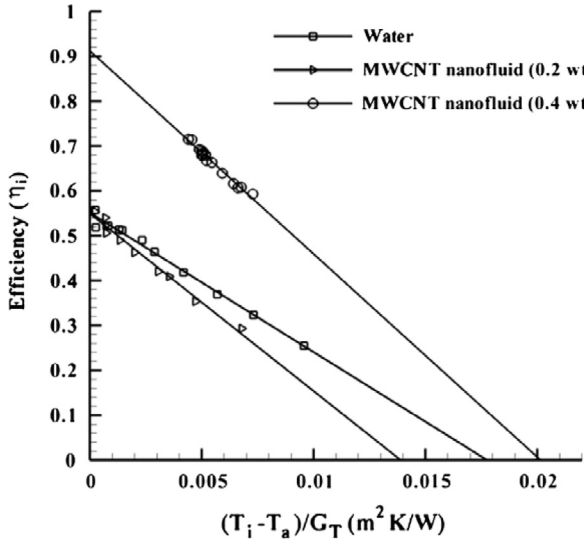

Fig. 8. The efficiency of solar collector for MWCNT nanofluids without surfactant and for water in the same mass flow rate [36].

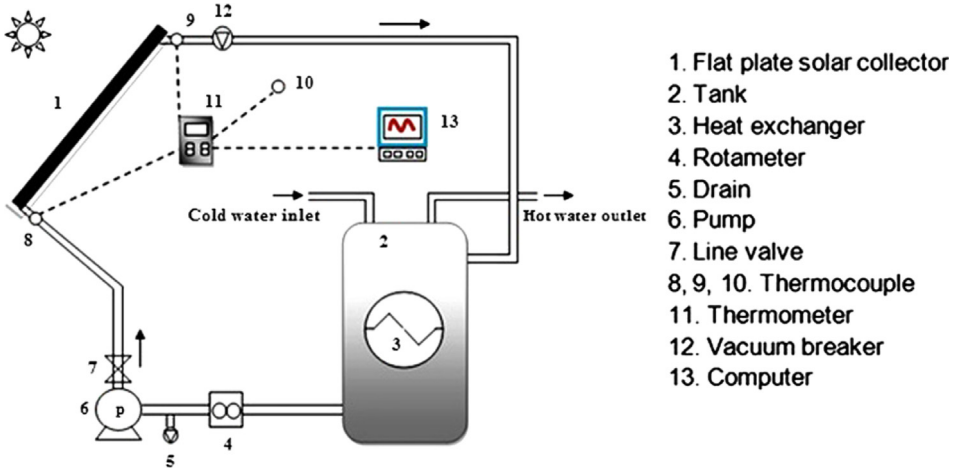

Fig. 7. The schematic of the experiment [35].

Yousefi et al. [37] investigated the effect of pH of MWCNT–H_2O nanofluid on the efficiency of a flat-plate solar collector. The experiments were carried out using 0.2 wt% MWCNT with various pH values (3.5, 6.5, and 9.5) and with Triton X-100 as additive. The ASHRAE standard was followed for testing the thermal performance of flat-plate solar collector. They found that increasing or decreasing the pH with respect to the pH of the isoelectric point can enhance the positive effect of nanofluids on the efficiency of the solar collector. Larger differences between the pH of nanofluids and that of isoelectric point enhance the efficiency of the collector (Fig. 9). Therefore, as the nanofluids become more acidic or basic, the positive effect of nanofluids on the efficiency of flat plate solar collector becomes higher.

Chougule et al. [38] fabricated the experimental set up of flat plate collectors using heat pipes. The effects of nanofluids as working fluid and solar tracker on solar heat pipe collector were analyzed. In each set up, three identical wickless copper heat pipes with a length of 620 mm and an outer diameter of 18 mm were used. The nanoparticles used were CNTs 10 nm to 12 nm in diameter. They found that the concentration of nanoparticles used in the preparation of nanofluid was 0.15% by volume, which indicates that a very low quantity of nanoparticles can improve the performance without incurring a high cost. Nanofluids increase the average efficiency of the solar heat pipe collector irrespective of change in tilt angle. Nanofluids with solar heat pipe collector gives better performance at higher tilt angle. The performance can be improved by locating the solar heat pipe collector at the place where the angle of obtaining the maximum total solar radiation matches with the higher performance tilt angle of the solar heat pipe collector. The solar tracking system adds an advantage to improve the efficiency in both water as well as nanoworking fluid solar heat pipe collector and also each of tilt angles for the solar heat pipe collector. During winter, heat pipes with solar water heater show better performance, that is, solar heat pipe collector should be used in cold climatic conditions.

Tiwari et al. [39] presented a comprehensive overview on the thermal performance of solar flat plate collector for water heating using different nanofluids. The effect of using the Al_2O_3 nanofluid as an absorbing medium in a flat-plate solar collector was investigated. The effect of mass flow rate and particle volume fraction of the efficiency of the collector was investigated. The results show that using the 1.5% (optimum) particle volume fraction of Al_2O_3 nanofluid increases the thermal efficiency as well as $kgCO_2$/kWh saving in hybrid mode of solar collector compared with water as working fluid by 31.64%.

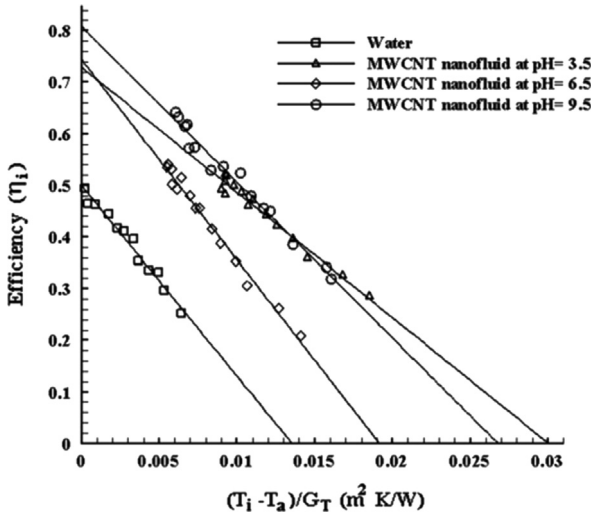

Fig. 9. The efficiency of the flat-plate solar collector with MWCNT nanofluids as base fluid at three pH values as compared with water in 0.0333 kg/s mass flow rate [37].

4.2. Direct absorption solar collector

Otanicar and Golden [40] determined the environmental and economic effects of using nanofluids to enhance solar collector efficiency as compared with conventional solar collectors for domestic hot water systems. For the current cost of nanoparticles, nanofluid-based solar collector has a slightly longer payback period but has the same economic savings as a conventional solar collector. A nanofluid-based collector has a lower embodied energy (~9%) and approximately 3% higher levels of pollution offsets than a conventional collector. The solar-weighted absorption coefficient for fluid's baseline capacity for absorbing solar energy was investigated. Results showed that water is the best absorber among the four tested liquids, namely, water, EG, propylene glycol, and therminol VP-1 [41].

Tyagi et al. [42] studied theoretically the capability of using a nonconcentrating direct absorption solar collector (DAC) and compared its performance with that of a conventional flat-plate collector. In Tyagi research, a nanofluid mixture of water and aluminum nanoparticles was used as the absorbing medium. According to the results of Tyagi, the efficiency of a DAC using nanofluids as the working fluid is up to 10% higher than that of a flat-plate collector.

Otanicar et al. [43] investigated the use of nanofluid-based in direct absorption solar collectors. They found that mixing nanoparticles in a liquid (nanofluids) dramatically affects the liquid thermophysical properties, such as thermal conductivity. Nanoparticles can improve the radiative properties of liquids and increase the efficiency of direct-absorption solar collectors. The experimental results on solar collectors were based on nanofluids from various nanoparticles (carbon nanotubes, graphite, and silver). They demonstrate efficiency improvements of up to 5% in solar thermal collectors by utilizing nanofluids as the absorption mechanism. The experimental and numerical results demonstrate that the efficiency initially rapidly increases with volume fraction and then stabilizes as the volume fraction continues to increase. The addition of small amounts of nanoparticles results in a rapid enhancement in the efficiency from the pure fluid case until a volume fraction of approximately 0.5%. With 20 nm silver particles, an efficiency improvement of 5% can be achieved (Fig. 10). As shown in figure, reducing the particle size further leads to an even greater enhancement in efficiency through the dependence of the optical properties on particle size.

Taylor et al. [44] reported that power tower solar collectors could benefit from the potential efficiency improvements that

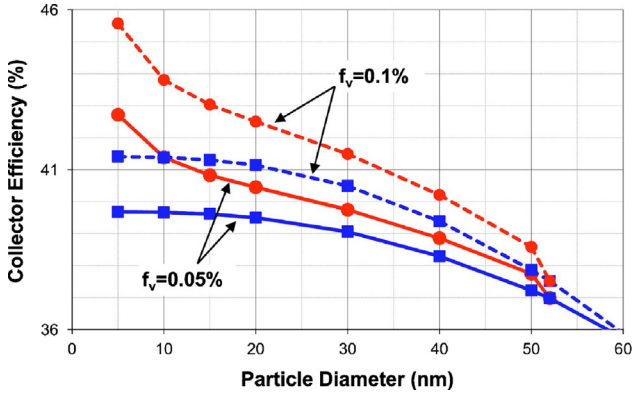

Fig. 10. Collector efficiency as a function of silver nanoparticle diameter (squares: bulk properties; circles: size-dependent properties) and volume fraction [43].

arise from using a nanofluid as a working fluid. A notional design of this type of nanofluids receiver was presented. Using this design, they had shown a 10% increase in theoretical nanofluid efficiency compared with surface-based collectors when solar concentration ratios range from 100 to 1000. Experiments on laboratory-scale nanofluid dish receiver suggest that up to 10% increase in efficiency is possible under optimal operating conditions.

Khullar and Tyagi [45] examined the potential of nanofluid-based concentrating solar water heating system (NCSWHS) as an alternative to systems based on fossil fuels. The paper reports a quantitative assessment to assess the potential environmental benefits that could be obtained from NCSWHS if substituted for those using fossil fuels. The analysis reveals that considerable emission reductions (approximately 2.2×103 kg of CO_2/household/year) and fuel savings can be achieved by using NCSWHS.

Saidur et al. [46] analyzed the effect of using nanofluids as working fluid on direct solar collector. The extinction coefficient of water-based aluminum nanofluids was evaluated under different nanoparticle sizes and volume fractions. Aluminum nanoparticles showed the highest extinction coefficient at a short wavelength and a peak at 0.3 μm. Aluminum nanoparticles can be used to enhance the light absorption ability of water at the visible and shorter wavelength region. Particle size shows minimal influence on the optical properties of nanofluids, whereas extinction coefficient is linearly proportionate to volume fraction. Although the extinction coefficient of nanofluids was independent of the nanoparticle size, the size should be controlled to be below 20 nm. The transmissivity of light was compared between pure water (base fluid) and nanofluids. The improvement was promising; with only 1.0% volume fraction, the nanofluids were almost opaque to light wave. A volume fraction of 1.0% shows satisfactory improvement to solar absorption; therefore, aluminum nanofluids were deemed a good solution for direct solar collector compared with the others.

He et al. [47] prepared Cu–H_2O nanofluids through a two-step method. The transmittance of nanofluids over solar spectrum (250 nm to 2500 nm) Factors (such as particle size, mass fraction, and optical path) influencing transmittance of nanofluids were investigated. The extinction coefficients measured experimentally were compared with the theoretical calculated value. The photothermal properties of nanofluids were also investigated. The transmittance of Cu–H_2O nanofluids is considerably less than that of deionized water. In addition, it decreases with increasing nanoparticle size, mass fraction, and optical depth. The highest temperature of Cu–H_2O nanofluids (0.1 wt%) can be up to 25.3% compared with deionized water. The good absorption ability of Cu–H_2O nanofluids for solar energy indicates that it is suitable for direct-absorption solar thermal energy systems.

4.3. Evacuated tube solar collector

Lu et al. [48] designed an especial open thermosyphon device used in high-temperature evacuated tubular solar collectors. The indoor experimental research was carried out to investigate the thermal performance of the open thermosyphon using deionized water and water-based CuO nanofluids as working liquid. The effects of mass flow rate, base fluid type, nanoparticle mass concentration, and operating temperature on the evaporating heat transfer characteristics in the open thermosyphon were investigated and discussed. Substituting water-based CuO nanofluids for water as the working fluid can significantly enhance the thermal performance of the evaporator, and evaporating heat transfer coefficients may increase by approximately 30% compared with those of deionized water. The mass concentration of CuO nanoparticles has a remarkable influence on the heat transfer coefficient in the evaporation section. In addition, the mass concentration of 1.2% corresponds to the optimal heat transfer enhancement (Fig. 11).

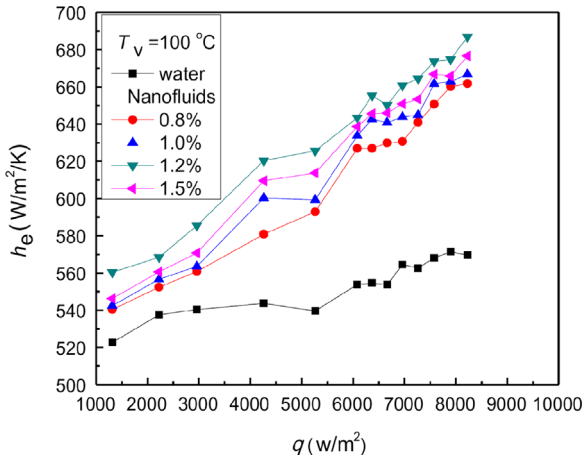

Fig. 11. Effect of the filling ratio on the evaporating HTC [48].

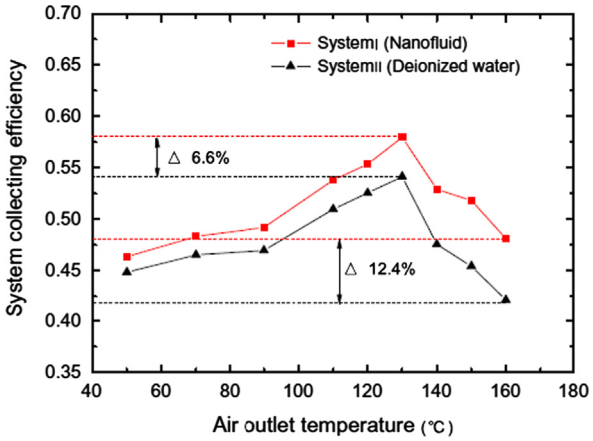

Fig. 12. Solar collecting efficiency under different operating temperatures [49].

Liu et al. [49] designed a novel evacuated tubular solar air collector integrated with simplified compound parabolic concentrator (CPC) and special open thermosyphon using water-based CuO nanofluid as working fluid to provide air with high and moderate temperatures. They found that the air outlet temperature and system collecting efficiency of the solar air collector using nanofluids as working fluid are higher than when water is used as working fluid. The collector was integrated with thermosyphon using water as the working fluid. The maximum value and the mean value of the collecting efficiency of the collector with open thermosyphon using nanofluids can increase by 6.6% and 12.4%, respectively (Fig. 12). Its maximum air outlet temperature exceeds 170 °C at the air volume rate of 7.6 m^3/h in winter (Fig. 13), even though the experimental system consists of only two collecting panels Their results show that the solar collector integrated with open thermosyphon has greater collecting performance than that integrated with the common concentric tube.

4.4. Parabolic trough collector

Risi et al. [50] modeled and optimized transparent parabolic trough collector (TPTC) based on gas-phase nanofluids. The use of directly radiated nanoparticles allows compensating the relatively low heat transfer coefficient typical of gaseous heat transfer fluids with an increased exchange surface. In addition, a proper mixture of CuO and Ni nanoparticles has been designed to allow a complete absorption of the solar energy within the transparent

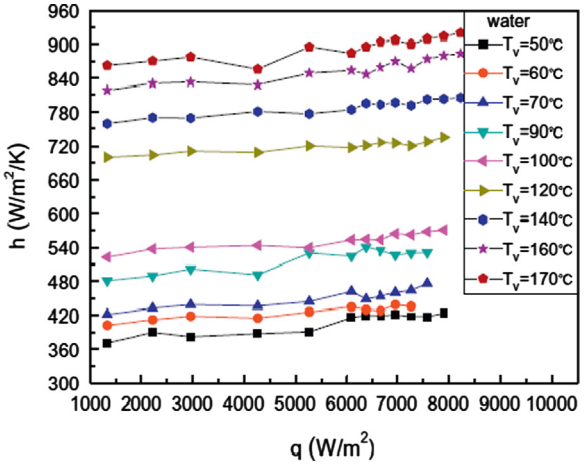

Fig.13. Evaporating HTC of water in thermosyphon under different operating temperatures [49].

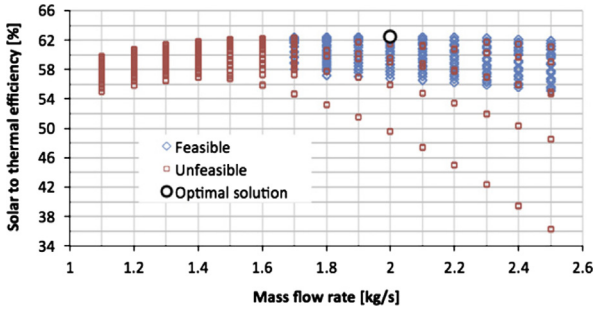

Fig. 14. Solar to thermal efficiency as a function of nanofluids mass flow rate [50].

receiver tube. Fig. 14 shows the solar-to-thermal efficiency as a function of nanofluid mass flow rate. Solar-to-thermal efficiency increases up to a maximum value (62.5%) with the increase in mass flow rate and gradually decreases up to the investigated limit of 2.5 kg/s. Simulations showed that TPTC solar-to-thermal efficiency is 62.5% at 650 °C nanofluid outlet temperature and 0.3% nanoparticle volume concentration.

Nasrin et al. [51] numerically investigated the influence of Prandtl number on free convection flow phenomena in a solar collector with glass cover plate and sinusoidal absorber. They used water–Al_2O_3 nanofluid as the working fluid. Comprehensive average Nusselt number, average temperature, and mean velocity inside the collector were presented as a function of the governing parameter. They found that the structure of the fluid streamlines and isotherms within the solar collector significantly depends on the *Pr*. Moreover, Fig. 15(i) and (ii) shows the Nu_c, Nu_r, and θ_{av} for the effect of Prandtl number *Pr*. Mounting *Pr* enhances the average Nusselt number for both convection and radiation. The rate of convective heat transfer increases by 26% and 18% for nanofluid and base fluid, respectively, whereas this rate for radiation is 8% with the increase in *Pr* from 1.73 to 6.62. Mean temperature decreases for both fluids with the increase in average heat transfer. Average velocity field increases with the decrease in *Pr* value. The increase in heat transfer rate is found to be more effective in water–Al_2O_3 nanofluids than in the base fluid.

4.5. Concentrated-parabolic solar collectors

Lenert et al. [52] presented a combined modeling and experimental study to optimize the efficiency of liquid-based solar receivers seeded with carbon-coated absorbing nanoparticles. They experimentally investigated a cylindrical nanofluid volumetric receiver, and showed good agreement with the model with varying optical thicknesses of the nanofluids. The efficiency of nanofluid volumetric receivers increases with increasing solar concentration and nanofluid height. Receiver-side efficiencies are predicted to exceed 35% when nanofluid volumetric receivers are coupled to a power cycle and optimized with respect to the optical thickness and solar exposure time. Their study provides an important perspective in the use of nanofluids as volumetric receivers in concentrated solar applications.

Khullar et al. [53] harvested solar radiant energy with the use of nanofluid-based concentrating parabolic solar collectors (NCPSC). The results of the model were compared with the experimental results of conventional concentrating parabolic solar collectors under similar conditions. While maintaining the same external conditions, the NCPSC shows approximately 5–10% higher efficiency than the conventional parabolic solar collector. Parametric studies were conducted to determine the influence of various parameters on NCPSC performance and efficiency. The theoretical results indicate that the NCPSC has the potential to utilize solar radiant energy more efficiently than a conventional parabolic trough. The performance of nanofluid solar collector is also summarized in Table 3.

5. PV/T collector

Solar energy has attracted significant attention because of its cleanness and availability. Solar energy can be used in different photovoltaic and photothermal applications. Photovoltaic application is the main means to convert solar radiation into electricity. Solar cells absorb solar radiation and convert it into electricity through photoelectric conversion.

In general, only 5–20% of the incident solar radiation can be converted into electricity and the rest is either reflected back or absorbed by the solar cells as heat. During summer, the temperatures of solar cells can reach 70 °C, which led to the following two problems: increase in saturation current and decrease in open voltage of the solar cells; and reduction of the silicon energy gap, thereby decreasing the efficiency of solar cells.

Solar PV/T applications can provide heat and electricity and thus improve the overall efficiency of solar energy. To achieve high efficiency and more power and heat from the PV/T system, cooling the PV cell is necessary, particularly in the areas with hot and humid climate. Based fluid (water) on PV/T collector is more desirable and effective than the existing air systems. Temperature fluctuation in the base fluid (water) of PV/T is much less than the air-based PV/T collectors, which are subjected to varying solar radiation levels.

Numerous studies have been conducted about the PV/T system with the use of water and air (working fluid) as heat removal media for different applications. Therefore, the use of nanofluids to cool the PV/T system may be reasonable. Investigate performance of PV/T system with the use of nanofluids to cool the PV panel and improve the thermal, electrical, and overall efficiencies is recommended. Nanofluids are stable suspensions prepared by dispersing nanoparticles into the base fluid. Given the small-scale effect, nanoparticle optical properties may have significant difference compared with pure water. Nanofluids have been widely used because of their enhanced thermal conductivities.

6. Water-type PV/T collector

The most common working fluid in liquid-based PV/T collectors are water and water/air; which is the most widely studied system [54].

6.1. Glazed and unglazed

Zondag et al. [55] and Jong [56] have conducted a series of comparisons between different types of PV/T design and different

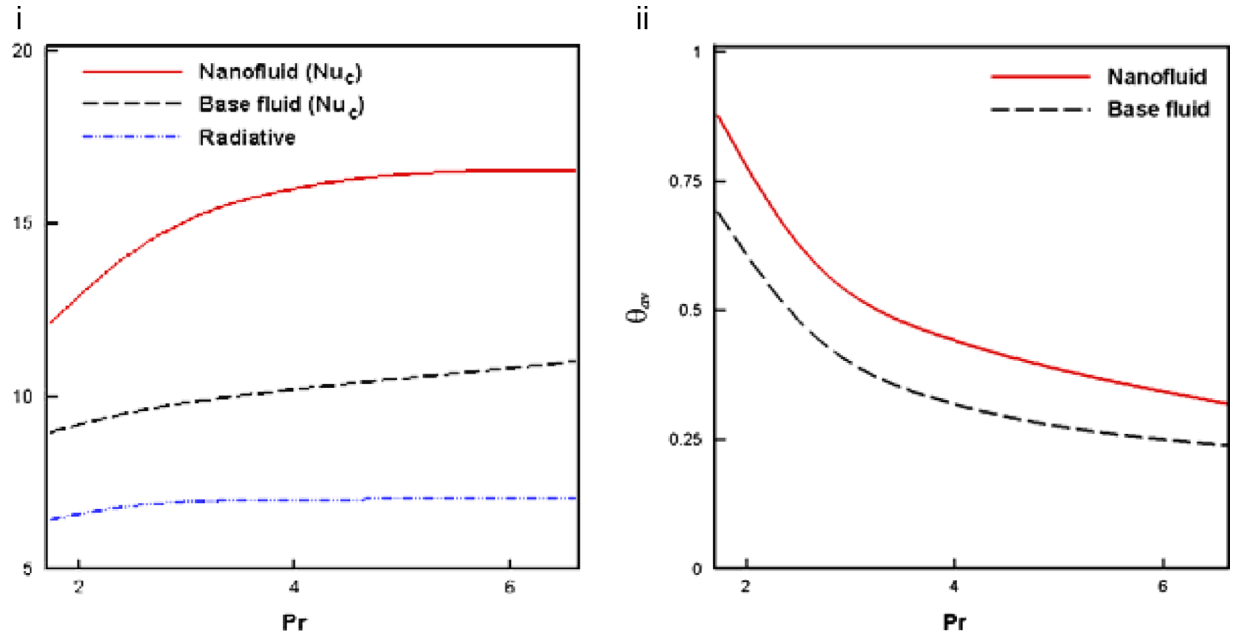

Fig. 15. Effect of *Pr* on (i) *Nu* (ii) θ_{av} [51].

types of thermal systems. Their experiments generally investigated the covered and uncovered PV/T and thermal systems with and without heat pump. Their studies indicated that an uncovered PV/T shows improved efficiency with the use of PV/T for low-temperature ground storage integrated with a heat pump.

Chow et al. [57] presented a flat-box-type hybrid collector under forced flow condition; simulation experiments were performed to study the steady-state performance of the collector under three different situations. Case A: the absorber was fully covered with PV module. Case *B*: the absorber was 50% covered with PV module. Case C: the absorber was not covered with PV module. They found that Case A shows thermal efficiency of 57.4% under zero reduced temperature condition, with a corresponding cell efficiency of 12.3% (or electrical efficiency of 11.5% based on the collector plate area), which is significant considering the simple design of this collector type. However, for Case C, the thermal efficiency can be improved with the use of selective absorber surface with low emissivity.

Tiwari and Sodha [58] evaluated the performance of hybrid PV/T water/air heating system under four configurations, namely, (a) unglazed with tedlar (UGT), (b) glazed with tedlar (GT) (Fig. 16), (c) unglazed without tedlar (UGWT), and (d) glazed without tedlar (GWT). They obtained the following results: (i) UGWT [case (c)] shows better performance at lower operating temperature. (ii) GT shows better performance at high operating temperature. (iii) IPVTS system with water as the working fluid shows better performance except for UGWT. The obtained overall thermal efficiencies of the IPVTS system for summer and winter conditions are approximately 65% and 77%, respectively.

Tiwari and Sodha [59] also evaluated the performance of solar PV/T system experimentally. Numerical computations were conducted for climatic data and design parameters of an experimental IPVTS system. The simulations predict a daily thermal efficiency of approximately 58%, which is close to the experimental value (61.3%) obtained by Huang et al. [60]. They found that the overall thermal efficiency of IPVTS increased from 24% (0.09/0.38) to 58% because of the additional thermal energy produced by the water flow.

Fraisse et al. [61] applied water hybrid PV/T collectors to combi-systems of Direct Solar Floor in Macon, France. Fig. 17 shows the general diagram of the installation. Four different configurations were studied. Case 1 (PV+T): consists of two 16 m^2 separate collectors. The thermal solar collector was conventional with glass cover. PV module was cooled by natural ventilation on its two faces. Case 2 (Uncov-PV/T): hybrid solar PV/T collector without glass cover and with a PV module surface of high emissivity (ε=0.9) and a global solar radiation absorption coefficient α=0.8. Its considered area varies from 16 m^2 to –32 m^2. Case 3 (Cov-PV/T): hybrid solar PV/T collector with glass cover also from 16 m^2 to 32 m^2. Case 4 (Cov-LE-PV/T): hybrid solar PV/T collector with glass cover and the PV module has low emissivity ("LE") ε=0.4. The conventional configuration leads to 26.3% auxiliary energy savings. As for the hybrid solar collectors, the same level of energy savings is achieved for 35 m^2 of covered PVT (Cov-PV/T) and 29 m^2 of LE covered PV/T (Cov-LE-PV/T). Only the Cov-LE-PV/T solution reached an area lower than the global surface (32 m^2) for a conventional PV/T configuration.

Dubey and Tiwari [62] provided a detailed analysis of energy, exergy, and electrical energy yield of PV/T flat plate collector (Fig. 18) for five different cities of India. Annual thermal and electrical energy yield were evaluated for four different series and parallel combination of collectors for comparison purpose were considered under New Delhi conditions. Case A: collectors were partially covered by PV modules and connected in series. Case B: identical set of collectors fully covered by PV module and by glass cover were connected in series. Case C: collectors fully covered by PV module and connected in series. Case D: series and parallel combination of *N* identical sets of panels fully covered by PV. Case A is better in terms of thermal energy and case D is better in terms of electrical energy. The partially covered collectors (case A) were beneficial in terms of annualized uniform cost if the primary requirement of user was thermal energy yield.

Chow et al. [63] investigate the appropriate glass cover on a thermosyphon-based water-heating PV/T system (Figs. 19 and 20). The effects of six selected operating parameters were evaluated. The energetic efficiency of the glazed collector is always better than the unglazed collector. The exergetic efficiency of the unglazed collector is better than the glazed collector in specific ranges of the six parameters. The increase in PV cell efficiency, packing factor, the ratio of water mass to collector area, and wind velocity are favorable factors for unglazed PV/T system, whereas the increase in ambient temperature is a favorable factor for selecting a glazed PV/T system.

Table 3
Summary of performance of solar collector using nanofluids.

Author	Type of collector	Type of nanofluids	Particle size (nm)	Volume fraction (%)	Results
Yousefi et al. [35]	Flat-plate	Al_2O_3 /water	15 nm	0.2, 0.4	For 0.2 wt% the efficiency increases up to 28.3% The surfactant causes an enhancement in heat transfer efficiency is 15.63%
Yousefi et al. [36]	Flat-plate	MWCNT/water	10–30 nm	0.2, 0.4	The 0.2 wt% MWCNT nanofluids without surfactant decrease the efficiency and to surfactant increase it Collector efficiency increases with increase the volume fraction compared with water
Yousefi et al. [37]	Flat-plate	MWCNT/water	10–30 nm	0.2 wt%	The more differences between the pH of nanofluids and pH of isoelectric point cause the more enhancements in the efficiency of the collector
Chougule et al. [38]	Flat-plate	CNT/water	D=10–12. L=0.1–10 μ	0.15 wt%	At 50° tilt angle both working fluids gave better performance as compared to the standard normal angle in both conditions Average collector efficiencies for water and nanoworking fluid are increased 12% and 11% at 31.50° tilt angle, while 7% and 4% respectively at 50° tilt angle using the tracking system
Tiwari et al. [39]	Flat-plate	Al_2O_3 /water	–	0.5–2 wt%	Using the 1.5% particle volume fraction of Al_2O_3 nanofluid increases the thermal efficiency as well as $kgCO_2$/kWh saving in a hybrid mode of solar collector in comparison with water as the working fluid by 31.64%
Otanicar and Golden [40]	Direct absorption	Graphite/water, EG	–	0.1 wt%	Using nanofluids solar collector leads to approximately 3% higher levels of pollution offsets than a conventional solar collector
Tyagi et al. [42]	Direct Absorption	Al_2O_3 /water	Less than 20 nm	0.1–5 wt%	The efficiency of a DAC using nanofluid is up to 10% higher than that of a flat-plate collector. Efficiency increases for nanofluids up to 2 wt%
Otanicar et al. [43]	Direct Absorption	CNT, graphite, and silver/water	D=6–20 & L=1–5×10^3 nm, D=30, D=20–40 nm	0–1 wt%	For 30 nm graphite, a maximum improvement, over a conventional flat surface absorber, of 3% With 20 nm silver an efficiency improvement of 5% An enhancement in the efficiency compared with pure water until 0.5 with. %
Taylor et al. [44]	Direct absorption	Graphite, Al_2O_3, Cu /therminol VP-1	20 nm	0.1 wt%	Enhancement in efficiency of up to 10% as compared to surface-based collectors
Saidur et al. [46]	Direct absorption	Al_2O_3/water	1, 5, 10, 20	2 wt%	1.0% showing satisfactory improvement to solar absorption, aluminum nanofluids was a good solution for direct solar collector compared to others
He et al. [47]	Direct absorption	CuO/water	20, 50 nm	0.01, 0.02, 0.04, 0.1, 0.2 wt%	The transmittance of Cu–H_2O nanofluids was much less than water, and decreases with increasing nanoparticle size, mass fraction and optical depth. The highest temperature of Cu–H_2O nanofluids (0.1 wt%) can increase up to 25.3% compared with water
Lu et al. [48]	Evacuated tubular	CuO/water	50 nm	0.8–1.5 wt%	Enhance the thermal performance of the evaporator and evaporating HTC increase by about 30% compared with those of deionized water The HTC in the evaporation section and the 1.2 wt% corresponds to the optimal heat transfer enhancement
Liu et al. [49]	Evacuated tubular	CuO/water	50 nm	1.2 wt%	The solar collector integrated with open thermosyphon has a much better collecting performance Increase the collecting efficiency, max and mean value increase to 6.6% and 12.4%, respectively
Risi et al. [50]	Transparent parabolic trough	(0.25% CuO, 0.05% Ni)/water	–	0.01–0.3	The optimization procedure find a maximum solar to thermal efficiency equal to 62.5%, for a nanofluids outlet temperature of 650 °C and a nanoparticles volume concentration of 0.3%
Nasrin et al. [51]	Glass cover plate and sinusoidal absorber	Al_2O_3/water	–	5 wt%	The Al_2O_3 nanoparticles with the highest *Pr* were established to be most effective in enhancing performance of heat transfer rate than base fluid
Lenert et al. [52]	Concentrated parabolic	C–Co/VP-1	10–100 nm	–	Efficiency increases with increasing nanofluids height and solar flux. The optimum optical thickness foe a non-selective receiver is 1.7
Khullar et al. [53]	Concentrated parabolic	Al_2O_3/VP-1	5 nm	–	The NCPSC has the potential to harness solar radiant energy and higher efficiency about 5–10% as compared to the conventional parabolic solar collector

Dubey and Tiwari [64] designed and tested an integrated combined system of a PV/T (glass–glass) solar water heater with 200 liter capacity, in outdoor condition for composite climate in New Delhi. Two flat plate collectors connected in series, each having an effective area of 2.16 m^2, were considered. A glass-to-glass PV module with an effective area of 0.66 m^2 was integrated at the bottom of one of the collector. A cross-sectional view of a combined PV/T solar water heating system is shown in Fig. 21. A significant increase in the instantaneous efficiency from 33% to 64% from case A to case C is found because of the increase in glazing area. The PV/T flat plate

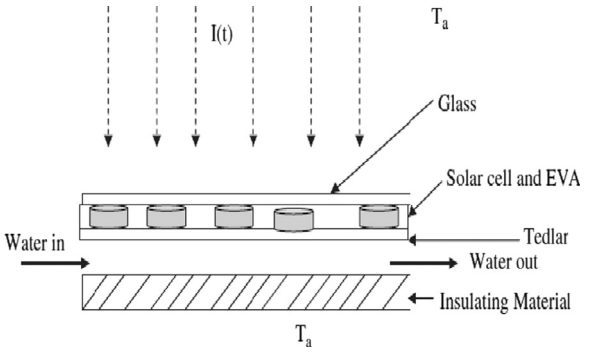

Fig. 16. Cross-sectional view of an integrated photovoltaic/thermal system [58].

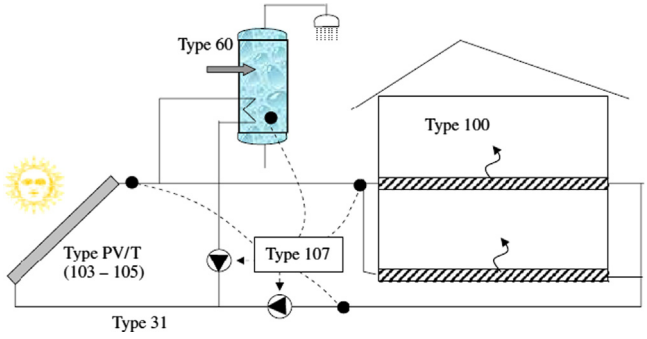

Fig. 17. Shows the general diagram of the installation [61].

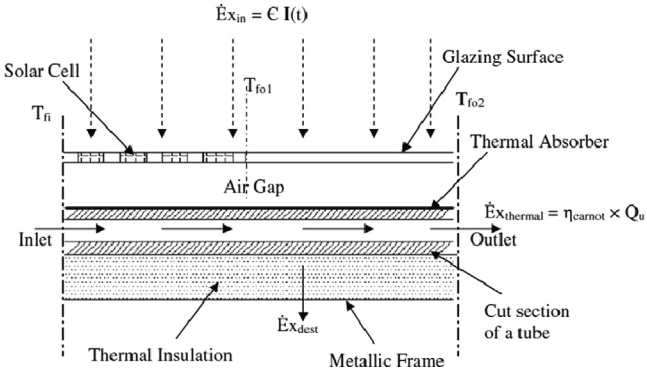

Fig. 18. Cross sectional side view of a flat plate collector partially covered by PV [62].

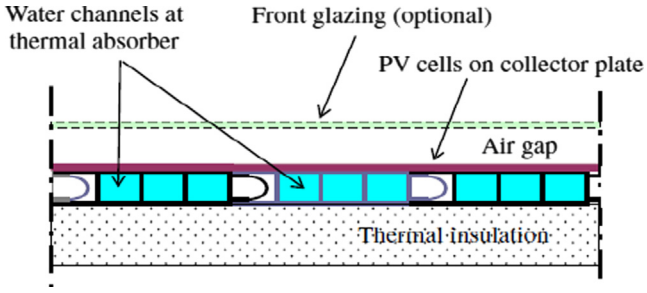

Fig. 19. Cross-section view of PV/T collector with flat-box absorber and multi-water channel design [63].

collector partially covered with PV module shows better thermal and average cell efficiency.

Joshi et al. [65] evaluated the thermal performance of a hybrid PV/T air collector system and analyzed two types of PV module, namely, PV module with glass-to-tedlar and glass-to-glass for composite climate of New Delhi. A schematic view of the PV/T

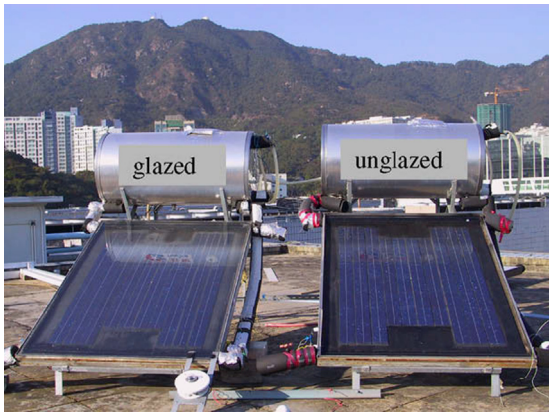

Fig. 20. PV/T collectors with and without glass cover [63].

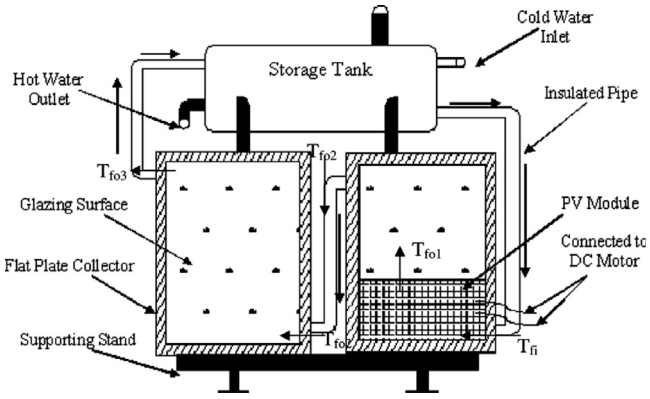

Fig. 21. Cross sectional view of a combined photovoltaic thermal (PV/T) solar water heating system [64].

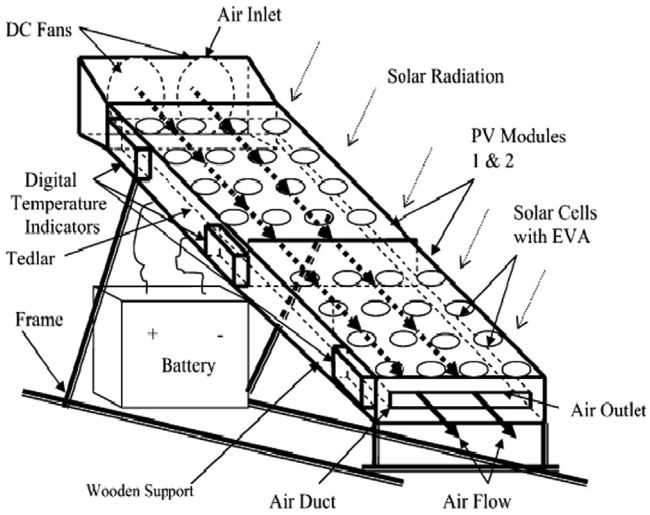

Fig. 22. Schematic diagram of hybrid PV/T air collector [65].

air collector is shown in Fig. 22. They found that the back surface temperature is higher in glass-to-glass PV/T air collector than in glass-to-tedlar PV/T air collector. The hybrid air collector with PV module glass-to-glass exhibits better performance in terms of overall thermal efficiency. Overall thermal efficiency of glass-to-glass PV/T air collector is better compared with glass-to-tedlar PV/T air collector. Overall thermal efficiency decreases with increase in length of the duct in both cases and increases with the increase in the velocity of duct air.

Erdil et al. [66] constructed and studied a hybrid system composed of a PV module and a solar thermal collector for energy collection at a geographic location in Cyprus. In this experimental study, they used only two PV modules with approximately 0.6 m^2 area. PV modules absorb a considerable amount of solar radiation that generates undesirable heat. Measurements based on electrical characteristics and water pre-heating show that the hybrid module is economically attractive. Electrical energy generation loss was well offset by a large gain in thermal energy collected by the circulating water.

6.2. Performance of PV/T collector

Zondang et al. [67] presented several steady-state and dynamic simulation models for water PV/T collector. A dynamic 3D model and steady 3D, 2D, and 1D models have been built, together with a first non-optimized prototype of the Combi-panel (Fig. 23). For the calculation of the daily yield, the simple 1D steady-state model performs almost as good as the much more time-consuming 3D dynamical model. They concluded that the 2D and 3D models are important for further optimization of the Combi-panel, which is a main target in the ongoing research.

Chow [68] proposed an explicit dynamic model based on the control-volume finite-difference method. The appropriateness of the nodal scheme has been tested using both steady-state and dynamic simulations. The model is suitable for hourly analysis of equipment energy performance. With an extension of the nodal scheme to include multi-dimensional thermal conduction on PV and absorber plates, the model is able to perform complete energy analysis on the hybrid collector.

Saitoh et al. [69] described the effectiveness of a hybrid solar collector. Experiments and analyses on power and heat generation characteristics of the hybrid solar collector were conducted. The efficiency of the hybrid solar collector was compared with those of a PV and a solar collector, and they found that the hybrid collector had an advantage in terms of exergy efficiency; however, some decrease in collector efficiency is also found. The hybrid system is expected to reduce panel installation area by approximately 27%. The PV/T collector is found to be better in terms of exergy efficiency.

PV/T systems are installed for residential use. To investigate the actual condition of the residential building, the PV/T systems were installed on the roof top of a residential building. Ji et al. [70] installed a 40 m^2 PV/T collector on a facade of the residential building in Hong Kong to investigate the difference between the thin film and crystalline silicon PV cell. The thermal efficiency of the thin film is found to be 48%, whereas that of the crystalline silicon is 43%. They proposed that the system can be utilized for pre-heating of hot water for residents in that building. The systems can provide cooling for the building with absorption of heat by the wall of building reduced during the PV/T system operation. They concluded that the hybrid system has potential to be widely used in a sub-tropical city such as Hong Kong.

Zakharchenko et al. [71] investigated the performance of the different panels in the hybrid PV/T system. Different kinds of PV panel materials, such as crystalline (c-) Si, α-Si, and $CuInSe_2$ thin film, were used in solar cell for the thermal contact between the panel and the collector. Different materials and constructions for the thermal contact between the panel and the collector were also evaluated. A prototype of the optimized panel for the hybrid PV/thermal system was built using the metallic substrate covered with thin insulating layer. They found that the power of the PV panel increased by 10% with the collector in the new hybrid system.

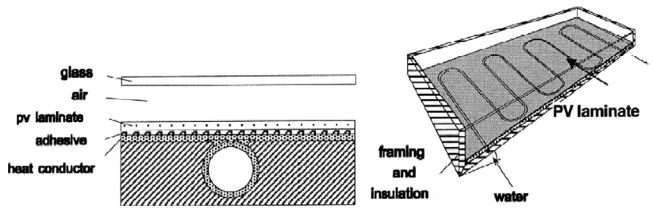

Fig. 23. The combi-panel [67].

Kalogirou and Tripanagnostopoulos [72] modeled and simulated a PV/T thermosyphon for three different locations, namely Nicosia (Cyprus), Athens (Greece), and Madison (USA). Polycrystalline and amorphous silicon solar cells were analyzed. The obtained electrical production values of the system using polycrystalline solar cells were 532, 515, and 499 kWh, and the solar thermal contributions were 0.686, 0.564, and 0.293 for the three locations, respectively. A non-hybrid PV system produces 30% more electrical energy, but they found that the hybrid PV/T system proved to supply a large percentage of the hot-water needs of a house.

Kalogirou and Tripanagnostopoulos [73] investigated TRNSYS simulation results for hybrid PV/T solar systems for domestic hot-water applications both passive (thermosyphonic) and active. Prototype models made from polycrystalline silicon and amorphous silicon PV module types combined with water heat extraction units were evaluated in terms of their electrical and thermal efficiencies. The simulation results were performed at different latitudes for the three locations: Nicosia (35°), Athens (38°), and Madison (43°). The electrical production of the system using polycrystalline solar cells is higher than that using the amorphous ones, but the solar thermal contribution is slightly lower. A non-hybrid PV system produces approximately 38% more electrical energy.

Vokas et al. [74] conducted a theoretical study of a PV/T system for domestic heating and cooling. The performances of the PV/T collector in terms of the variation in geographical region and different total surface areas of the system were analyzed. They found that the PV/T system with total surface area of 30 m^2 was 47.79% and 25.03%. They found that a PV/T collector can produce remarkable amounts of thermal energy, which can be used to cover a remarkable part of the domestic heating and cooling load.

Bernardo et al. [75] evaluated the performance of low concentrating PV/T system used in a validated simulation model that estimates the hybrid outputs in different geographic locations. The method includes a comparison of the hybrid performance with conventional collectors and photovoltaic modules working side-by-side. The obtained measurements are 6.4% hybrid electrical efficiency, 0.45 optical efficiency, and 1.9 $W/m^2\,°C$ *U*-value. These values are less than the parameters of standard PV modules and flat plate collectors. A margin of improvement is found for the studied hybrid, but this combination results in difficulties in concentrating hybrids to compete with conventional PV modules and flat plate collectors.

Chow et al. [76] investigated the annual performance of building-integrated PV/water-heating (PVW) system for warm climate in Hong Kong. The prediction was performed with the use of numerical models and verified by experimental data under natural and forced circulation modes. The simulation results indicate that this system performs better under natural circulation mode than the forced circulation mode because the pumping power can be saved. The obtained year-average thermal and cell conversion efficiencies were 37.5% and 9.39%, respectively. The two modes of operation were able to reduce the thermal transmission through the PVW wall by approximately 72% and 71%, respectively. The payback period of the installation is estimated to be 14 years. The economic advantage of the BiPVW system is found to be significantly better than the BiPV system.

Boubekri et al. [77] studied the combination of the collector with a PV module as an efficient method for improving the system

performance, particularly the electrical and thermal performance. The mathematical model was based on the energy transfer phenomenon within the various components of the collector. They found that the thermal properties of the adhesive layer are important in the thermal and electrical efficiency of the collector and the use of materials with good thermal conductivity results in an increase in solar conversion. The increase in the inclination angle causes a reduction in the incidental direct solar radiation intensity on the collector, thereby reducing the electrical power.

Gang et al. [78] proposed a novel heat pipe PV/T system that could simultaneously supply electrical and thermal energy. Compared with a traditional water-type PV/T system, the heat pipe PV/T system can be used in cold regions without becoming frozen. A dynamic model of the heat pipe PV/T system was presented, and a test rig was constructed. The performances of the heat pipe PV/T system were investigated under different parametric conditions, such as water flow rates, tube space of heat pipes, and kinds of solar absorptive coatings of the absorber plate, and total PV/T efficiencies of the HP-PV/T system enhance with the increase in water flow rate. The effect of water flow rate on heat gain was more significant than on electrical gain. The HP-PV/T system that used collectors with solar absorptive coating can increase heat gain and total PV/T efficiencies but decrease electricity output.

Kamthania et al. [79] evaluated the performance of a hybrid semitransparent PV/T double pass facade for space heating in New Delhi, India. The thermal model was developed with the use of the energy balance equations of the proposed hybrid PV/T double pass facade under quasi-steady state condition. They found that the annual thermal and electrical energy were 480.81 and 469.87 kWh, respectively. The yearly overall thermal energy generated by the system is 1729.84 kWh. The room air temperature increases by 5–6 °C than the ambient air temperature for a typical winter day. The proposed double pass air facade is most useful in space heating for buildings.

Tiwari et al. [80] evaluated the performance of the PV module integrated with air duct for composite climate in India. Thermal and electrical energy were generated by a PV module with higher efficiency. They derived an analytical expression for an overall efficiency (electrical and thermal) using energy balance equation for each component. The experimental and theoretical results are consistent for back surface, outlet air, and top surface temperatures with a correlation coefficient of 0.97–0.99 and root mean square percent deviation of 7.54–13.89%. An 18% increase in an overall efficiency of hybrid PV/T system is achieved because of the available thermal energy in addition to electrical energy. The overall thermal efficiency of the PV/T system was significantly increased because of the use of thermal energy in PV module.

Zhao et al. [81] presented the optimized design of a PV/T system using both non-concentrated and concentrated solar radiation. The system consists of a PV module with silicon solar cell and a thermal unit based on the direct absorption collector concept. The thermal unit absorbs 89% of the infrared radiation for photothermal conversion and transmits 84% of visible light to the solar cell for photoelectric conversion. With the decrease in mass flow rate, the outflow temperature of the working fluid reaches 74 °C, whereas the temperature of the PV module remains at approximately 31 °C and the constant electrical efficiency is approximately 9.6%. Furthermore, when the incident solar irradiance increases from 800 W/m^2 to 8000 W/m^2, the system generates 196 °C working fluid with constant thermal efficiency of approximately 40%, the exergetic efficiency increases from 12% to 22%, and the electrical efficiency slightly decreases from 9.8% to 7.3%.

Joshi et al. [82] evaluated the effect of colors of light on the PV/T system performance in terms of energy and exergy. A case study was conducted to validate the model with the use of solar radiation data in four different months, namely, January, April, August, and October for New Delhi, India. They found that the new proposed photonic theory is consistent with the exergy analysis based on the second law of thermodynamics. The energy of the solar radiation received on the PV surface showed a fair agreement with the energy levels at the red and orange ranges of the visible spectrum.

6.3. Design absorber of PV/T collector

Zondag et al. [83] studied nine different design concepts of combined PV/T water solar collector systems. Fig. 24 shows the common configurations of currently used PV/T systems. The designs shown in Fig. 24a indicate the concept of sheet-and-tube PV/T collector. The PV/T collector channel, free-flow PV/T collector, and related two absorber PV/T collectors are shown in Fig. 24b, c and d, respectively. They obtained 52% thermal efficiency for an uncovered PV/T collector and 58% for single cover sheet-and-tube design. Analysis from all designs concept showed that the single cover sheet-and-tube collector is the optimal design with significantly easier manufacturing process.

He et al. [84] developed a water-type hybrid collector with a polycrystalline PV module on a flat-box type aluminum alloy thermal absorber (Fig. 25). The energy performance of the developed system is encouraging. The daily thermal efficiency was approximately 40%, which is approximately 0.8× that for a conventional solar thermosyphon collector system. In addition, the energy saving efficiency was better than the conventional system. Therefore, the product design has a good potential for domestic market.

Chow et al. [85] evaluated the performance of a new design of water-type PVT collector system (Figs. 26 and 27) A dynamic simulation model of the PVT collector system was developed and validated by the experimental measurements. They found that the type of collector has an annual average thermal efficiency of 38.1% and a payback period of 12 years for the PVT collector system, which is significantly shorter than that of the non-hybrid PV/T system.

Ji et al. [86] constructed and designed a flat-box aluminum-alloy photovoltaic and water-heating system for natural circulation. Outdoor tests of the improved prototype were conducted in a moderate climate zone. The PV/T water heating system was designed with natural circulation and experiments were conducted with different water masses and different initial water temperatures in an outdoor environment. They found that the daily electrical efficiency was approximately 10.15%, the characteristic daily thermal efficiency $>45\%$, the characteristic daily total efficiency was $>52\%$, and the characteristic daily primary energy saving could reach up to 65% for this system with a PV cell packing factor of 0.63 and front glazing transmissivity of 0.83.

Furthermore, a hybrid PV/T collector manufactured in a copolymer material and running in low flow rate conditions was developed (Fig. 28) by Cristofari et al. [87]. They studied the thermal and electrical performances of the solar system and found that the average efficiencies were 55.5% for thermal, 12.7% for PV, and 68.2% and 88.8%, respectively, for the total system efficiency and energy-saving efficiency. Thermal performances are important in the development of these systems. With approximately the same performances, a copolymer PV/T design for the solar collector may be good choice because of its weight reduction, easy installation, and low cost.

Touafek et al. [88] proposed a new PVT hybrid collector based on a new design approach, which aims to increase the energy effectiveness of electric and thermal conversion with the lowest cost compared with the existing conventional hybrid collector. The experimental and theoretical results are approximately similar, in

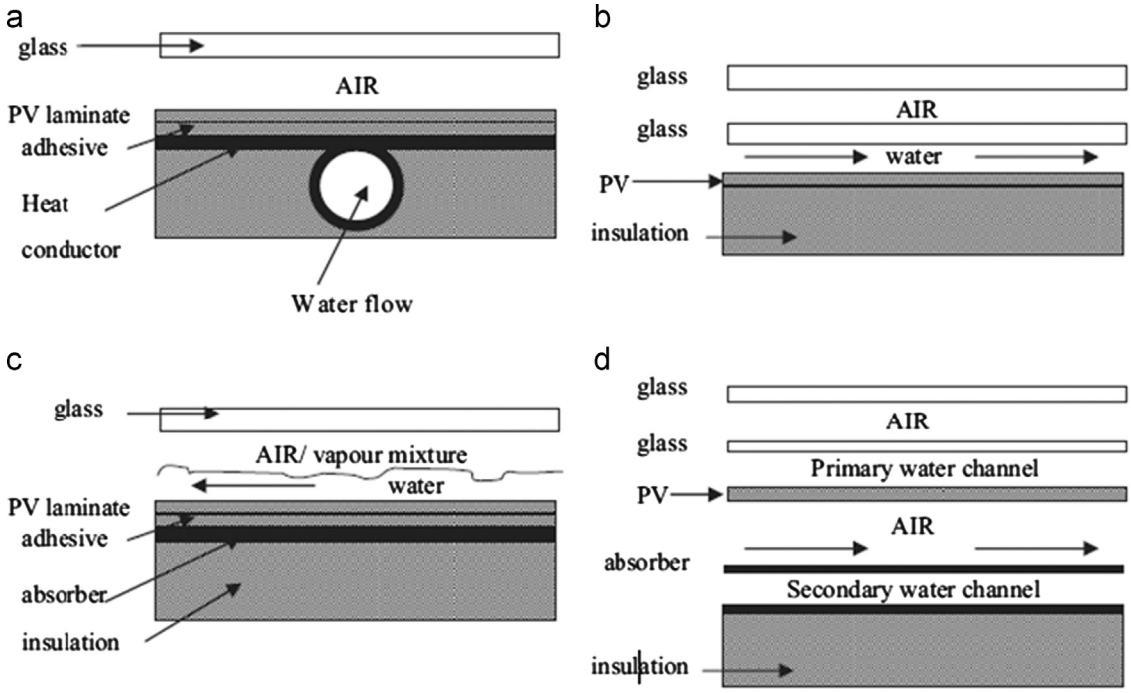

Fig. 24. Combined PV/T water collector [83].

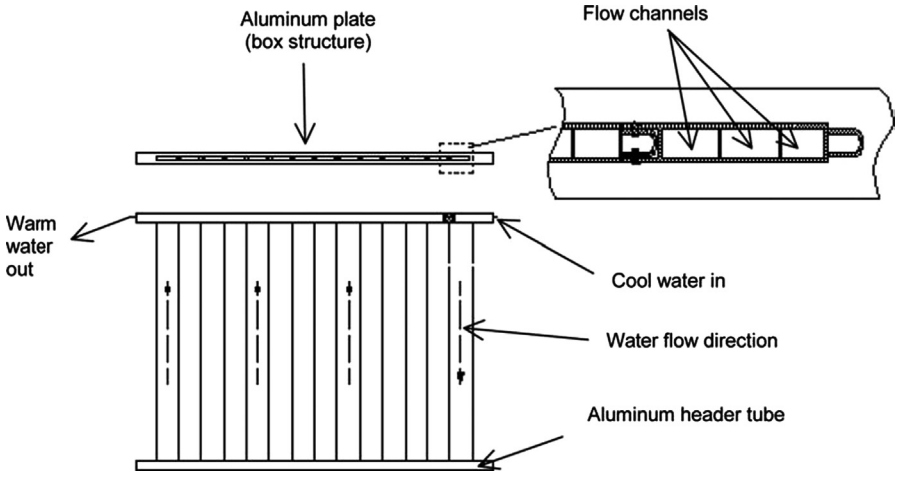

Fig. 25. Construction details of thermal absorber [84].

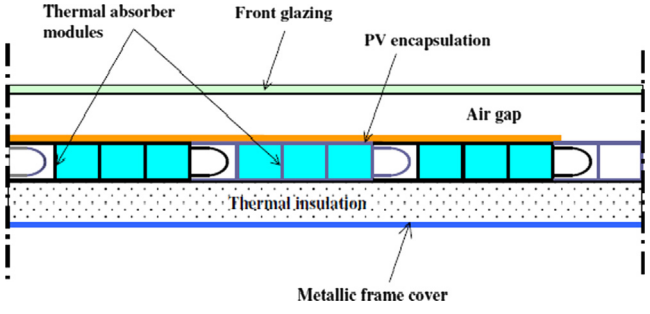

Fig. 26. Cross-section view of the PVT collector showing several integrated flat-box absorber modules (N.T.S.) [85].

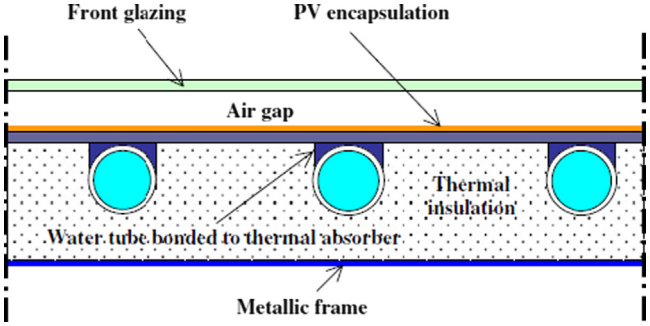

Fig. 27. Cross-section view showing three adjacent water tubing in a sheet and-tube PVT collector (N.T.S.) [85].

which the thermal performances of the new hybrid collector are improved compared with the classic hybrid collectors. This novel collector provides a new technical approach to maximize the total output of conversion with lower cost compared with the traditional hybrid collectors.

Daghigh et al. [89] investigated the performance of amorphous and crystalline silicon-based PV/T solar collectors. A new design concept of water-based PV/T collector were designed and evaluated for building-integrated applications, absorber plate, and PV

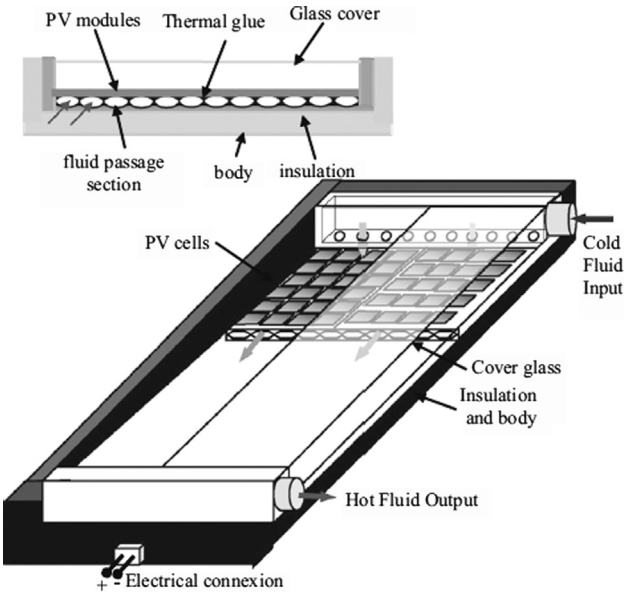

Fig. 28. The photovoltaic/thermal solar collector [87].

module. The results of simulation study of amorphous silicon (a-Si) PV/T and crystalline silicon (c-Si) module types were based on the metrological condition of Malaysia for a typical day in March. At a flow rate of 0.02 kg/s, solar radiation level between 700 and 900 W/m^2, and ambient temperature between 22 and 32 °C, the obtained electrical, thermal, and combined photovoltaic thermal efficiencies were 4.9%, 72%, and 77%, for the PV/T (a-Si), respectively, 11.6%, 51%, and 63% for the PV/T (c-Si). The overall efficiency of this new and simple design is significantly better than that of conventional absorber for both amorphous and crystalline silicon cells.

Charalambous et al. [90] developed a novel mathematical analysis for the cost of conventional fin and tube PV/T collectors. Optimizing absorber plate material of a conventional fin and tube PV/T collector leads to a substantial reduction in material content. Based on the absorber plate design consideration, if the efficiency factor F' of PV/T collector is constant, the useful collected heat Q_u of the PV/T collector is also constant. They found that the thermal performance reduces by approximately 7% with electricity production of the serpentine PV/T prototype. Moreover, the serpentine prototype thermal performance was higher by approximately 4% than the corresponding performance of the header and the riser prototype in with and without electricity production.

Gang et al. [91] simulated the heat-pipe PV/T (HP-PV/T) systems with regard to electrical and thermal energy. The annual electrical and thermal behavior of the HP-PV/T system were predicted and analyzed in three typical climate areas of China, namely, Hong Kong, Lhasa, and Beijing. They found that the system with auxiliary heating, when used in Hong Kong, Lhasa, and Beijing, the annual thermal energy were 1665.05 MJ/m^2 to 1872.22 MJ/m^2, 2939.67 MJ/m^2 to 3328.25 MJ/m^2, and 2111.07 MJ/m^2 to 2352.95 MJ/m^2, respectively; the annual electrical energy produced were 261.32 MJ/m^2 to 264.98 MJ/m^2, 462.14 MJ/m^2 to 466.1 MJ/m^2, and 322.84 MJ/m^2 to 328.15 MJ/m^2, respectively. For the system without auxiliary heating, the annual thermal and electrical energy were lower than those of the system with auxiliary heating. Based on the HP-PV/T system with auxiliary heating equipment, the daily solar energy was insufficient to cover the daily hot-water load. Thus, auxiliary energy is needed to cover the hot-water load. The system with small water storage capacity obtains less thermal energy than that with large water storage capacity.

Wei and Chen [92] presented a theoretical analysis of novel PV/T solar collector. The collector was made of vacuum tube-PV sandwich, in which the water that passes through U-shape cooper tube of the collector extracts the heat from PV panel, thereby reducing the PV cell working temperature. This phenomenon improves the electrical and thermal efficiencies of the PV cells. They found that the thermal efficiency slightly increases, whereas the electrical efficiency decreases slightly with the increase in radiation. Both the thermal and electrical efficiencies increase by 1.4% and 0.23%, respectively, with every 10 kg/h increase in water mass flow, and decrease by 3.8% and 0.6%, respectively, with every 10 °C increase in inlet water temperature.

6.4. Exergy and energy analysis of PV/T collector

Fujiwa and Tani [93] conducted exergy analysis to evaluate the experimental performance of a PV/T system because exergy can be used to qualitatively compare the thermal with electrical energy based on the same standard. Fig. 29 shows that the coverless PV/T collector produces high electrical exergy and Fig. 30 shows that thermal exergy of the coverless PV/T is the lowest among the systems considered. Flow rate affects the performance of PV/T system because of the increase in water velocity in the tube results in the increase in heat transfer coefficient, thereby enhancing the cooling on the PV panel or collector.

Tiwari et al. [94] investigated an analytical expression for the water temperature of an integrated PV/T solar (IPVTS) water heater under constant flow rate hot water withdrawal. The analysis was extended for hot water withdrawal at constant collection temperature. The overall exergy efficiency initially increases and then starts to decrease, thereby indicating the optimum value of flow rate is 0.006 kg/s. However, thermal efficiency increases significantly with the increase in flow rate up to 0.006 kg/s and then increase is marginal.

Joshi et al. [95] investigated the performance of the PV and PV/T system in terms of energy and exergy efficiencies. Two different methods for assessing efficiencies of a PV system were developed

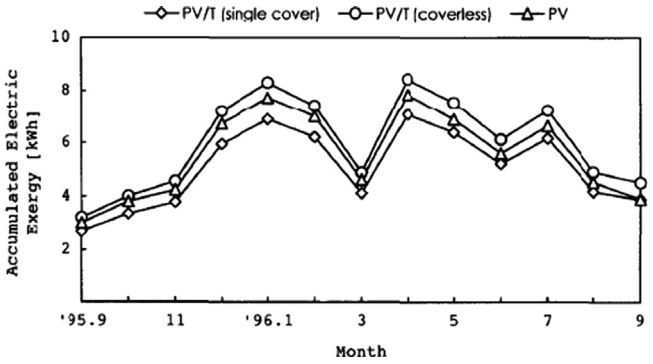

Fig. 29. Monthly changes of available energy gain by exergetic evaluation on electrical [93].

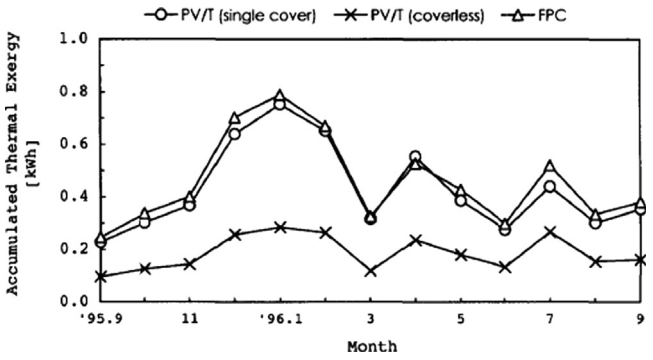

Fig. 30. Monthly changes of available energy gain by exergetic evaluation on thermal [93].

and applied to an actual system. The fill factor is important in determining the behavior of the exergy efficiency of PV systems. Higher fill factor results in higher exergy efficiency. They found that the energy efficiency varies from a minimum of 33% to a maximum of 45%, and the corresponding exergy efficiency (PV/T) varies between 11.3% and of 16%, whereas the exergy efficiency (PV) varies (7.8–13.8%). At the actual exergy efficiency, the fill factor ranges between 0.55 and 0.75. Better exergy efficiency is obtained with higher fill factor values.

Dubey and Tiwari [96] evaluated the overall thermal energy and exergy provided in the form of heat and electricity from hybrid PV/T solar water heating system considering five different cases with and without withdrawals. The annual heat and electricity were evaluated by considering the four types of weather conditions in five different cities of India (New Delhi, Bangalore, Mumbai, Srinagar, and Jodhpur). The annual maximum heat and electricity were obtained in case (ii) (energy: 4263.2 kWh and exergy: 529.7 kWh) and minimum in case (v) (energy: 1038.8 kWh and exergy: 196.9 kWh) compared with all of the other cases under New Delhi condition. Annual maximum and minimum energy gains and efficiency were obtained from Jodhpur and Srinagar City, respectively. This type of configuration (hybrid PV/T) is significantly useful in the remote and urban areas, where electricity and hot water can be obtained simultaneously.

A different exergy efficiency correlations of solar PV/T system were presented by Wu et al. [97] Performance evaluation results of a certain PV/T hybrid system were inconsistent with each other when different correlations of exergy efficiency are used. The overall output was higher for a given PV/T collector than the outputs of two separated PV and solar thermal systems placed side-by-side. Unlike PV system, PV/T system uses the thermal energy available on the PV panel, the thermal energy gain can be utilized as useful energy and thus the desirable exergy of PV/T system becomes the sum of the electrical and thermal exergies. At low solar radiation intensity, the exergy efficiency of PV/T system equals the electrical efficiency of the reference conditions. Exergy analysis with regard to the temperature difference between the cell and ambient on the premise shows that no heat loss results in higher exergy.

Rajoria et al. [98] conducted an overall thermal energy and exergy analysis for different configurations of hybrid PV/T array. The hybrid PV/T array consists of a series and parallel combinations of 36 PV modules. On the basis of this transient model, an appropriate hybrid PVT array was selected for different climatic conditions (Bangalore, Jodhpur, New Delhi, and Srinagar). They found that the configuration under case-II exhibits better results in terms of overall thermal energy gain, which was 12.1% higher than that of case-III, but the overall exergy gain for case-III was 12.9% higher than that of case-II. The overall thermal energy and exergy gain for Bangalore was 4.54×10^4 and 2.07×10^4 kWh, respectively, which are the highest among the cities investigated.

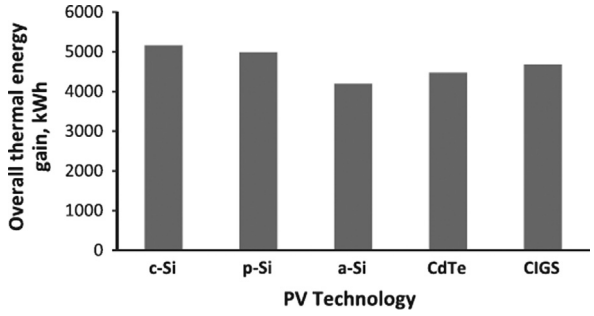

Fig. 31. Annual overall thermal energy gain with different PV technology [99].

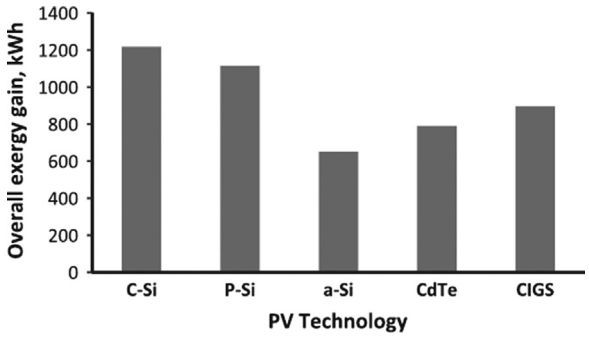

Fig. 32. Annual overalsl exergy gain with different PV technology [99].

Mishra and Tiwari [99] evaluated and compared the energy matrices of a hybrid PV/T (HPVT) water collector under constant collection temperature mode with five different types of PV modules, namely, c-Si, p-Si, a-Si (thin film), CdTe, and CIGS. The analysis was based on overall thermal energy and exergy outputs from HPVT water collector. They found that c-Si PV module was the optimum alternative for electrical power production. As shown in Figs. 31 and 32, the maximum annual overall thermal energy and exergy were obtained for c-Si PV module. The energy production factor (EPF) and life cycle conversion efficiency (LCCE) of HPVT water collector using five different types of PV modules for life time (T)= 10, 15 and 20 years of the system are discussed. EPF and LCCE increase with the increase in T of the system for all of the PV module types.

Mishra and Tiwari [100] presented the analysis of HPVT water collectors under constant collection temperature mode. The analysis was conducted in terms of thermal energy, electrical energy, and exergy gain for two different configurations, namely, case *A* (collector partially covered with PV module) and case *B* (collector fully covered with PV module) compared with the conventional flat plate collector (FPC). They found that case *A* was more favorable with regard to thermal energy, whereas case *B* was suitable for electricity generation. On the basis of the numerical calculations, the annual thermal energy gain was found to be 4167.3 and 1023.7, and the annual net electrical energy gain was 320.65 and 1377.63 for cases *A* and *B*, respectively. The annual overall thermal energy gain decreased by 9.48% and an annual overall exergy gain increased by 39.16% from case *A* to case *B*. Percent deviations of 1.6%, 18.6%, and 59.4% were found in the overall thermal efficiency for FPC, case *A*, and case *B*, respectively.

7. Conclusion

Nanotechnology allows the production of nano-scaled particles. The suspensions of these particles in conventional fluids have created a new type of heat-transfer fluid. Nanofluids are being given significant interest in thermal engineering. This paper presents an overview of the recent developments in the study of heat transfer and solar collector with the use of nanofluids. Nanofluids containing small amounts of nanoparticles have substantially higher thermal conductivity than base fluids. The thermal conductivity enhancement of nanofluids depends on the volume fraction, size, type of nanoparticles and base fluid. Suspended nanoparticles remarkably increased the forced convective heat transfer performance of base fluid. At the same Reynolds number, the heat transfer of the nanofluids increases with the increase the volume fraction of nanoparticles and decrease in nanoparticles size.

This paper presents an overview of studies about the performance of solar collector, such as flat-plate and direct solar-absorption

collectors with the use of nanofluids as working fluid. The effect of surface-to-volume ratio on thermal conductivity is more than the effect of the surface size of nanoparticles.

This paper reviewed the recent development in various PV/T systems. The review covers water PV/T collector types, analytical models, as well as simulation and experimental studies. The parameters affecting PV/T performance, such as covered versus uncovered PV/T collectors, are also considered. An efficiency fact is introduced in this paper to provide a general understanding for designers and researchers. The most promising PV/T application in residential applications is found to be the flat-plate geometry in collector design. The fluid on the thermal side of PV/T is generally liquid, air, or their combination.

Among the different liquids, water is affordable (less than air), clean, and available. However, for specific application in which special configuration or design must be applied, the use of other liquids may be needed. The sheet and tube collector is highly efficient and less expensive in practical application of water-based PV/T, such as building-integrated systems. A review of the literature shows that many studies have been conducted about the potential of nanofluids for cooling of different thermal systems. Therefore, nanofluids can be used to cool PV/T systems.

References

[1] Sopian K, Liu HT, Kakac S, Veziroglu TN. Performance of a double pass photovoltaic thermal solar collector suitable for solar drying systems. Energy Convers Manag 2000;41:353–65.

[2] Johansson TB, Kelly H, Reddy AKN, Williams RH. Renewable energy – sources for fuels and electricity; 1993.

[3] Sani E, Barison S, Pagura C, Mercatelli L, Sansoni P, Fontani D, et al. Carbon nanohorns-based nanofluids as direct sunlight absorbers. Opt Express 2010;18:5179–87.

[4] Wong KV, De Leon O. Applications of nanofluids: current and future. Adv Mech Eng 2010;2010:1–11.

[5] Kern EC, Russell MC. Combined photovoltaic and thermal hybrid collector systems. In: Proceedings of the 13th IEEE photovoltaic specialists conference. Washington DC, USA; 1978.

[6] Wang X, Xu X, Choi SUS. Thermal conductivity of nanoparticle-fluid mixture. J Thermophys Heat Transf 1999;13:474–80.

[7] Eastman J, Choi U, Li S, Thompson L, Lee S Enhanced thermal conductivity through the development of nanofluids. In: Proceedings of materials research society symposium. Cambridge Univ Press; 1997. p. 3–12.

[8] Lee S, Choi S-S, Li S, Eastman J. Measuring thermal conductivity of fluids containing oxide nanoparticles. J Heat Transf 1999;121:280–9.

[9] Xuan Y, Li Q. Heat transfer enhancement of nanofluids. Int J Heat Fluid Flow 2000;21:58–64.

[10] Eastman J, Choi S, Li S, Yu W, Thompson L. Anomalously increased effective thermal conductivities of ethylene glycol-based nanofluids containing copper nanoparticles. Appl Phys Lett 2001;78:718–20.

[11] Xie H, Wang J, Xi T, Liu Y, Ai F, Wu Q. Thermal conductivity enhancement of suspensions containing nanosized alumina particles. J Appl Phys 2002;91:4568–72.

[12] Putra N, Thiesen P, Roetzel W. Temperature dependence of thermal conductivity enhancement for nanofluids. J Heat Transf 2003;125:567–74.

[13] Hong T-K, Yang H-S, Choi C. Study of the enhanced thermal conductivity of Fe nanofluids. J Appl Phys 2005;97:064311–4.

[14] Murshed S, Leong K, Yang C. Enhanced thermal conductivity of TiO_2–water based nanofluids. Int J Therm Sci 2005;44:367–73.

[15] Li CH, Peterson G. Experimental investigation of temperature and volume fraction variations on the effective thermal conductivity of nanoparticle suspensions (nanofluids). J Appl Phys 2006;99:084314–8.

[16] Hwang YJ, Ahn YC, Shin HS, Lee CG, Kim GT, Park HS, et al. Investigation on characteristics of thermal conductivity enhancement of nanofluids. Curr Appl Phys 2006;6:1068–71.

[17] Lee J-H, Hwang KS, Jang SP, Lee BH, Kim JH, Choi SUS, et al. Effective viscosities and thermal conductivities of aqueous nanofluids containing low volume concentrations of Al_2O_3 nanoparticles. Int J Heat Mass Transf 2008;51:2651–6.

[18] Vajjha RS, Das DK. Experimental determination of thermal conductivity of three nanofluids and development of new correlations. Int J Heat Mass Transf 2009;52:4675–82.

[19] Mintsa HA, Gilles R, Tam NC, Dominique D. New temperature dependent thermal conductivity data for water-based nanofluids. Int J Therm Sci 2009;48:363–71.

[20] Wen D, Ding Y. Experimental investigation into convective heat transfer of nanofluids at the entrance region under laminar flow conditions. Int J Heat Mass Transf 2004;47:5181–8.

[21] Zhou DW. Heat transfer enhancement of copper nanofluid with acoustic cavitation. Int J Heat Mass Transf 2004;47:3109–17.

[22] Yang Y, Zhang ZG, Grulke EA, Anderson WB, Wu G. Heat transfer properties of nanoparticle-in-fluid dispersions (nanofluids) in laminar flow. Int J Heat Mass Transf 2005;48:1107–16.

[23] Ding Y, Alias H, Wen D, Williams RA. Heat transfer of aqueous suspensions of carbon nanotubes (CNT nanofluids). Int J Heat Mass Transf 2006;49:240–50.

[24] Zeinali Heris S, Nasr Esfahany M, Etemad SG. Experimental investigation of convective heat transfer of Al2O3/water nanofluid in circular tube. Int J Heat Fluid Flow 2007;28:203–10.

[25] Ding Y, Chen H, He Y, Lapkin A, Yeganeh M, Šiller L, et al. Forced convective heat transfer of nanofluids. Adv Powder Technol 2007;18:813–24.

[26] Jung J-Y, Oh H-S, Kwak H-Y. Forced convective heat transfer of nanofluids in microchannels. Int J Heat Mass Transf 2009;52:466–72.

[27] Fotukian SM, Nasr Esfahany M. Experimental investigation of turbulent convective heat transfer of dilute γ-Al_2O_3/water nanofluid inside a circular tube. Int J Heat Fluid Flow 2010;31:606–12.

[28] Fotukian SM, Nasr Esfahany M. Experimental study of turbulent convective heat transfer and pressure drop of dilute CuO/water nanofluid inside a circular tube. Int Commun Heat Mass Transf 2010;37:214–9.

[29] Sajadi AR, Kazemi MH. Investigation of turbulent convective heat transfer and pressure drop of TiO2/water nanofluid in circular tube. Int Commun Heat Mass Transf 2011;38:1474–8.

[30] Akhavan-Behabadi MA, Pakdaman MF, Ghazvini M. Experimental investigation on the convective heat transfer of nanofluid flow inside vertical helically coiled tubes under uniform wall temperature condition. Int Commun Heat Mass Transf 2012;39:556–64.

[31] Kayhani MH, Soltanzadeh H, Heyhat MM, Nazari M, Kowsary F. Experimental study of convective heat transfer and pressure drop of TiO_2/water nanofluid. Int Commun Heat Mass Transf 2012;39:456–62.

[32] Duffie JA, Beckman WA. Solar engineering of thermal processes. 3rd ed.. New Jersey: John Wiley & Sons; 2006.

[33] Hottel HC, Woertz BB. The performance of flat-plate solar heat collectors. Trans ASME 1942;64:94–102.

[34] Atlanta: ASHRAE; 2003.

[35] Yousefi T, Veysi F, Shojaeizadeh E, Zinadini S. An experimental investigation on the effect of Al_2O_3–H_2O nanofluid on the efficiency of flat-plate solar collectors. Renew Energy 2012;39:293–8.

[36] Yousefi T, Veisy F, Shojaeizadeh E, Zinadini S. An experimental investigation on the effect of MWCNT-H_2O nanofluid on the efficiency of flat-plate solar collectors. Exp Therm Fluid Sci 2012;39:207–12.

[37] Yousefi T, Shojaeizadeh E, Veysi F, Zinadini S. An experimental investigation on the effect of pH variation of MWCNT–H_2O nanofluid on the efficiency of a flat-plate solar collector. Sol Energy 2012;86:771–9.

[38] Chougule SS, Pise AT, Madane PA. Performance of nanofluid-charged solar water heater by solar tracking system. In: Proceedings of IEEE international conference on advances in engineering, science and management (ICAESM); 2012. p. 247–53.

[39] Tiwari AK, Ghosh P, Sarkar J. Solar water heating using nanofluids – a comprehensive overview and environmental impact analysis. Int J Emerg Technol Adv Eng 2013;3:221–4.

[40] Otanicar TP, Golden JS. Comparative environmental and economic analysis of conventional and nanofluid solar hot water technologies. Environ Sci Technol 2009;43:6082–7.

[41] Otanicar TP, Phelan PE, Golden JS. Optical properties of liquids for direct absorption solar thermal energy systems. Sol Energy 2009;83:969–77.

[42] Tyagi H, Phelan P, Prasher R. Predicted efficiency of a low-temperature nanofluid-based direct absorption solar collector. J Sol Energy Eng 2009;131:1–7.

[43] Otanicar TP, Phelan PE, Prasher RS, Rosengarten G, Taylor RA. Nanofluid-based direct absorption solar collector. J Renew Sustain Energy 2010;2:033102.

[44] Taylor RA, Phelan PE, Otanicar TP, Walker CA, Nguyen M, Trimble S, et al. Applicability of nanofluids in high flux solar collectors. J Renew Sustain Energy 2011;3:023104.

[45] Khullara V, Tyagia H. A study on environmental impact of nanofluid-based concentrating solar water heating system. Int J Environ Stud 2012;69:220–32.

[46] Saidur R, Meng TC, Said Z, Hasanuzzaman M, Kamyar A. Evaluation of the effect of nanofluid-based absorbers on direct solar collector. Int J Heat Mass Transf 2012;55:5899–907.

[47] He Q, Wang S, Zeng S, Zheng Z. Experimental investigation on photothermal properties of nanofluids for direct absorption solar thermal energy systems. Energy Convers Manag 2013;73:150–7.

[48] Lu L, Liu Z-H, Xiao H-S. Thermal performance of an open thermosyphon using nanofluids for high-temperature evacuated tubular solar collectors. Sol Energy 2011;85:379–87.

[49] Liu Z-H, Hu R-L, Lu L, Zhao F, Xiao H-S. Thermal performance of an open thermosyphon using nanofluid for evacuated tubular high temperature air solar collector. Energy Convers Manag 2013;73:135–43.

[50] de Risi A, Milanese M, Laforgia D. Modelling and optimization of transparent parabolic trough collector based on gas-phase nanofluids. Renew Energy 2013;58:134–9.

[51] Nasrin R, Parvin S, Alim MA. Effect of Prandtl number on free convection in a solar collector filled with nanofluid. Proc Eng 2013;56:54–62.

[52] Lenert A, Wang EN. Optimization of nanofluid volumetric receivers for solar thermal energy conversion. Sol Energy 2012;86:253–65.

[53] Khullar V, Tyagi H, Phelan PE, Otanicar TP, Singh H, Taylor RA. Solar energy harvesting using nanofluids-based concentrating solar collector. J Nanotechnol Eng Med 2013;3:1003–12.
[54] Ibrahim A, Othman MY, Ruslan MH, Mat S, Sopian K. Recent advances in flat plate photovoltaic/thermal (PV/T) solar collectors. Renew Sustain Energy Rev 2011;15:352–65.
[55] Zondag HA, Jong MJM, Van WGJH. Development and applications for PV thermal. In: 17th EPSEC; 2001. p. 2001.
[56] Jong MJM. System studies on combined PV/Thermal panels. In: 11th symposium thermische solarenergie. Staffelstein; 2001.
[57] Chow TT, He W, Ji J. Hybrid photovoltaic-thermosyphon water heating system for residential application. Sol Energy 2006;80:298–306.
[58] Tiwari A, Sodha MS. Performance evaluation of hybrid PV/thermal water/air heating system: a parametric study. Renew Energy 2006;31:2460–74.
[59] Tiwari A, Sodha MS. Performance evaluation of solar PV/T system: an experimental validation. Sol Energy 2006;80:751–9.
[60] Huang BJ, Lin TH, Hung WC, Sun FS. Performance evaluation of solar photovoltaic/thermal systems. Sol Energy 2001;70:443–8.
[61] Fraisse G, Ménézo C, Johannes K. Energy performance of water hybrid PV/T collectors applied to combisystems of Direct Solar Floor type. Sol Energy 2007;81:1426–38.
[62] Dubey S, Tiwari GN. Analysis of PV/T flat plate water collectors connected in series. Sol Energy 2009;83:1485–98.
[63] Chow TT, Pei G, Fong KF, Lin Z, Chan ALS, Ji J. Energy and exergy analysis of photovoltaic-thermal collector with and without glass cover. Appl Energy 2009;86:310–6.
[64] Dubey S, Tiwari GN. Thermal modeling of a combined system of photovoltaic thermal (PV/T) solar water heater. Sol Energy 2008;82:602–12.
[65] Joshi AS, Tiwari A, Tiwari GN, Dincer I, Reddy BV. Performance evaluation of a hybrid photovoltaic thermal (PV/T) (glass-to-glass) system. Int J Therm Sci 2009;48:154–64.
[66] Erdil E, Ilkan M, Egelioglu F. An experimental study on energy generation with a photovoltaic (PV)-solar thermal hybrid system. Energy 2008;33:1241–5.
[67] Zondag HA, Vries DWD, WGJV Helden, Zolingenr JCV. Steenhoven AAV. the thermal and electrical yield of a PV-thermal collector. Sol Energy 2002;72:113–28.
[68] Chow TT. Performance analysis of photovoltaic-thermal collector by explicit dynamic model. Sol Energy 2003;75:143–52.
[69] Saitoh H, Hamada Y, Kubota H, Nakamura M, Ochifuji K, Yokoyama S, et al. Field experiments and analyses on a hybrid solar collector. Appl Therm Eng 2003;23:2089–105.
[70] Ji J, Chow T-T, He W. Dynamic performance of hybrid photovoltaic/thermal collector wall in Hong Kong. Build Environ 2003;38:1327–34.
[71] Zakharchenko R. Photovoltaic solar panel for a hybrid PV/thermal system. Sol Energy Mater Sol Cells. 2004;82:253–61.
[72] Tripanagnostopoulos SKaY. Performance of a hybrid pv/t thermosyphon system. World Renew Energy Congr 2005:1162–7.
[73] Kalogirou SA, Tripanagnostopoulos Y. Hybrid PV/T solar systems for domestic hot water and electricity production. Energy Convers Manag 2006;47:3368–82.
[74] Vokas G, Christandonis N, Skittides F. Hybrid photovoltaic–thermal systems for domestic heating and cooling – a theoretical approach. Sol Energy 2006;80:607–15.
[75] Bernardo LR, Perers B, Håkansson H, Karlsson B. Performance evaluation of low concentrating photovoltaic/thermal systems: a case study from Sweden. Sol Energy 2011;85:1499–510.
[76] Chow TT, Chan ALS, Fong KF, Lin Z, He W, Ji J. Annual performance of building-integrated photovoltaic/water-heating system for warm climate application. Appl Energy 2009;86:689–96.
[77] Boubekri M, Chaker A, Cheknane A. Numerical approach for performance study of hybrid PV/thermal collector. Rev Energ Renouv 2009;12:355–68.
[78] Gang P, Huide F, Huijuan Z, Jie J. Performance study and parametric analysis of a novel heat pipe PV/T system. Energy 2012;37:384–95.
[79] Kamthania D, Nayak S, Tiwari GN. Performance evaluation of a hybrid photovoltaic thermal double pass facade for space heating. Energy Build 2011;43:2274–81.
[80] Tiwari A, Sodha MS, Chandra A, Joshi JC. Performance evaluation of photovoltaic thermal solar air collector for composite climate of India. Sol Energy Mater Sol Cells 2006;90:175–89.
[81] Zhao J, Song Y, Lam W-H, Liu W, Liu Y, Zhang Y, et al. Solar radiation transfer and performance analysis of an optimum photovoltaic/thermal system. Energy Convers Manag 2011;52:1343–53.
[82] Joshi AS, Dincer I, Reddy BV. Effect of colors of light on the PV/T system performance. Int J Energy Res 2012;36:572–8.
[83] Zondag HA, de Vries DW, van Helden WGJ, van Zolingen RJC, van Steenhoven AA. The yield of different combined PV-thermal collector designs. Sol Energy 2003;74:253–69.
[84] He W, Chow T-T, Ji J, Lu J, Pei G, Chan L-s. Hybrid photovoltaic and thermal solar-collector designed for natural circulation of water. Appl Energy 2006;83:199–210.
[85] Chow TT, He W, Ji J, Chan ALS. Performance evaluation of photovoltaic-thermosyphon system for subtropical climate application. Sol Energy 2007;81:123–30.
[86] Ji J, Lu J-P, Chow T-T, He W, Pei G. A sensitivity study of a hybrid photovoltaic/thermal water-heating system with natural circulation. Appl Energy 2007;84:222–37.
[87] Cristofari C, Notton G, Canaletti JL. Thermal behavior of a copolymer PV/Th solar system in low flow rate conditions. Sol Energy 2009;83:1123–38.
[88] Touafek K, Haddadi M, Malek A. Modelling and experimental validation of a new hybrid photovoltaic thermal collector. IEEE Trans Energy Convers 2011;26:176–83.
[89] Daghigh R, Ibrahim A, Jin GL, Ruslan MH, Sopian K. Predicting the performance of amorphous and crystalline silicon based photovoltaic solar thermal collectors. Energy Convers Manag 2011;52:1741–7.
[90] Charalambous PG, Kalogirou SA, Maidment GG, Yiakoumetti K. Optimization of the photovoltaic thermal (PV/T) collector absorber. Sol Energy 2011;85:871–80.
[91] Gang P, Huide F, Jie J, Tin-tai C, Tao Z. Annual analysis of heat pipe PV/T systems for domestic hot water and electricity production. Energy Convers Manag 2012;56:8–21.
[92] Wei P, Chen HB. Investigation on a novel PV/T solar collector. Adv Mater Res 2012;446–449:2873–8.
[93] Fujiwa T, Tani T. Annual exergy evaluation on photovoltaic thermal hybrid collector. Sol Energy Mater Sol Cells 1997;47:135–48.
[94] Tiwari A, Dubey S, Sandhu GS, Sodha MS, Anwar SI. Exergy analysis of integrated photovoltaic thermal solar water heater under constant flow rate and constant collection temperature modes. Appl Energy 2009;86:2592–7.
[95] Joshi AS, Dincer I, Reddy BV. Thermodynamic assessment of photovoltaic systems. Sol Energy 2009;83:1139–49.
[96] Dubey S, Tiwari GN. Energy and exergy analysis of hybrid photovoltaic/thermal solar water heater considering with and without withdrawal from tank. J Renew Sustain Energy 2010;2:043106, http://dx.doi.org/10.1063/1.3464754.
[97] Wu SY, Guo FH, Xiao l. Comparative study on exergy efficiency of solar photovoltaic/thermal (PV/T) system. Adv Mater Res 2011;347–353:476–80.
[98] Rajoria CS, Agrawal S, Tiwari GN. Overall thermal energy and exergy analysis of hybrid photovoltaic thermal array. Sol Energy 2012;86:1531–8.
[99] Mishra RK, Tiwari GN. Energy matrices analyses of hybrid photovoltaic thermal (HPVT) water collector with different PV technology. Sol Energy 2013;91:161–73.
[100] Mishra RK, Tiwari GN. Energy and exergy analysis of hybrid photovoltaic thermal water collector for constant collection temperature mode. Sol Energy 2013;90:58–67.